AGU PUBLICATIONS

Tectonics

RESEARCH ARTICLE
10.1002/2017TC004799

Key Points:
- Structural and geomorphological analysis constrain variations in architecture, segmentation, and evolution of the Main Ethiopian Rift
- More than half of the rift is asymmetric, with architecture and segmentation primarily controlled by the pre-rift lithospheric structure
- Asymmetric rifts directly progress to focused axial tectonic-magmatic activity, without transitioning into a symmetric rifting stage

Correspondence to:
G. Corti,
giacomo.corti@igg.cnr.it

Citation:
Corti, G., Molin, P., Sembroni, A., Bastow, I. D., & Keir, D. (2018). Control of pre-rift lithospheric structure on the architecture and evolution of continental rifts: Insights from the Main Ethiopian Rift, East Africa. *Tectonics*, *37*, 477–496. https://doi.org/10.1002/2017TC004799

Received 6 SEP 2017
Accepted 3 JAN 2018
Accepted article online 15 JAN 2018
Published online 8 FEB 2018

Control of Pre-rift Lithospheric Structure on the Architecture and Evolution of Continental Rifts: Insights From the Main Ethiopian Rift, East Africa

Giacomo Corti[1], Paola Molin[2], Andrea Sembroni[2], Ian D. Bastow[3], and Derek Keir[4,5]

[1]Istituto di Geoscienze e Georisorse, Consiglio Nazionale delle Ricerche, Florence, Italy, [2]Dipartimento di Scienze, Università degli Studi di Roma Tre, Rome, Italy, [3]Department of Earth Science and Engineering, Imperial College London, London, UK, [4]Ocean and Earth Science, University of Southampton, Southampton, UK, [5]Dipartimento di Scienze della Terra, Università degli Studi di Firenze, Florence, Italy

Abstract We investigate the along-axis variations in architecture, segmentation, and evolution of the Main Ethiopian Rift (MER), East Africa, and relate these characteristics to the regional geology, lithospheric structure, and surface processes. We first illustrate significant along-axis variations in basin architecture through analysis of simplified geological cross sections in different rift sectors. We then integrate this information with a new analysis of Ethiopian topography and hydrography to illustrate how rift architecture (basin symmetry/asymmetry) is reflected in the margin topography and has been likely amplified by a positive feedback between tectonics (flexural uplift) and surface processes (fluvial erosion and unloading). This analysis shows that ~70% of the 500 km long MER is asymmetric, with most of the asymmetric rift sectors being characterized by a master fault system on the eastern margin. We finally relate rift architecture and segmentation to the regional geology and geophysical constraints on the lithosphere. We provide strong evidence that rift architecture is controlled by the contrasting nature of the lithosphere beneath the homogeneous, strong Somalian Plateau and the weaker, more heterogeneous Ethiopian Plateau, differences originating from the presence of pre-rift zones of weakness on the Ethiopian Plateau and likely amplified by surface processes. The data provided by this integrated analysis suggest that asymmetric rifts may directly progress to focused axial tectonic-magmatic activity, without transitioning into a symmetric rifting stage. These observations have important implications for the asymmetry of continental rifts and conjugate passive margins worldwide.

Plain Language Summary The Ethiopian Rift Valley is a classic example of an area where a continent is splitting apart. Here active volcanism, earthquakes, and fracturing of the Earth's surface break continents and form new oceans. In this paper we analyze the shape and size of the faults and fractures combined with the relief and river drainage of the rift valley, in order to interpret which faults control the shape of the rift and how they have evolved through time. We find that more than half of the rift is defined by a large fault escarpment along the eastern side of the rift, with the western side defined by a gradual slope (an asymmetric rift). Less than half is a "classical" rift with clear fault escarpments on both sides (a symmetric rift), and we find no evidence for the previously held view of progressive evolution from an asymmetric to symmetric rift. Instead, we find that the morphology of the rift is primarily controlled by the contrasting properties of the rocks beneath the two sides of the rift, with major fault escarpments forming only where the rocks are strong.

1. Introduction

Continental rifts often have considerable along-strike variations in architecture and magmatism. Variations in fault pattern and evolution may be the result of variations in pre-existing lithospheric rheology, rift width, and extension rate and kinematics (e.g., Brune, 2016; Corti, 2012; Ebinger, 2005; Ziegler & Cloetingh, 2004). Along-axis differences in magmatism are commonly explained by processes such as variable mantle potential temperature, heterogeneous anomalous volatile content in the asthenosphere, variable extension rate, or processes such as melt focusing at steep gradients of the lithosphere-asthenosphere boundary (e.g., Keir et al., 2015 and references therein). Among these parameters, pre-existing plate structure is expected to play a major role in controlling continental rift architecture, because variations in crustal and lithospheric vertical layering and strength and/or the presence of inherited heterogeneities may significantly

influence the style and distribution of deformation at both local and regional scale (e.g., Brune, 2016; Corti, 2012; Sokoutis et al., 2007; Ziegler & Cloetingh, 2004). Continental rifting results from the application of extensional stresses to a predeformed, anisotropic lithosphere and, consequently, rift structures are not randomly distributed. They instead tend to follow the trend of pre-existing weaknesses (such as ancient orogenic belts), avoiding stronger regions such as cratons (e.g., Buiter & Torsvik, 2014; Dunbar & Sawyer, 1989; Tommasi & Vauchez, 2001; Vauchez et al., 1997; Versfelt & Rosendahl, 1989; Ziegler & Cloetingh, 2004). In these conditions, variations in the mechanical properties of the rifting plate (e.g., Scholz & Contreras, 1998) and/or the presence of the pervasive and/or discrete fabrics (e.g., Ring, 1994; Versfelt & Rosendahl, 1989) may exert a primary control on the extension-related pattern of faulting at both regional and local scales (e.g., Brune, 2016; Corti, 2012; Ziegler & Cloetingh, 2004). Recent studies support the strong influence played by along-axis variations in basement fabrics on rift segmentation, inducing significant variations in the characteristics of the rift margins (e.g., vertical throw on major boundary faults) and the symmetry or asymmetry of the rift basins (see for instance examples from Lake Malawi in Laó-Dávila et al., 2015, or from the Upper Rhine Graben in Grimmer et al., 2017). Differences in rift symmetry/asymmetry are also typically interpreted to be time-dependent: observations from the East African Rift System suggest a progression from asymmetric to symmetric rifting, eventually followed by axial focusing of the volcanism and faulting (e.g., Hayward & Ebinger, 1996; WoldeGabriel et al., 1990). Moreover, numerical modeling indicates that unloading related to fluvial incision enhances the flexural uplift at major rift escarpments, generating a positive feedback between tectonics and surface processes (Kooi & Beaumont, 1994; Petit et al., 2007; Tucker & Slingerland, 1994). Therefore, the dynamic coupling between flexural uplift and fluvial erosion may significantly influence the symmetric or asymmetric structure of the rift.

In this contribution, we integrate detailed geological-structural and geomorphological analysis to investigate the along-axis variations in architecture, segmentation, and evolution of the different rift sectors of the Main Ethiopian Rift (MER), East Africa, and relate these characteristics to the lithospheric structure and surface processes. The MER is a classical example of continental rifting developed within a highly anisotropic lithosphere that has experienced several tectonic events over the last one billion years of geological history and tectonics (e.g., Abbate, Bruni, & Sagri, 2015 and references therein). It is an ideal study locale for the analysis of rift structure in conjunction with surface processes since the expression of different stages in the evolutionary rift sequence, from initial rifting in the south to incipient breakup in the north, are all subaerially exposed and rigorously studied at depth using geophysical techniques (e.g., Corti, 2009; Ebinger et al., 2017; Keir et al., 2013). To investigate the variations in the characteristics of rifting in the MER, we first illustrate simplified geological cross sections in different portions of the rift, which show significant along-axis variations in the distribution of extension-related deformation and basin architecture. We then use new analysis of the topography and hydrography of the study area as an independent analysis of basin architecture, and to further investigate quantitatively the erosion-tectonic feedback and the response of surface processes to the variable rift architecture along the MER. We relate rift architecture and segmentation to the pre-rift rheology of the continental lithosphere and demonstrate a significant correlation between asymmetry (presence of half graben) of the MER and locally weak lithosphere on the side of the rift lacking a main border fault. We interpret an important influence exerted by the contrasting (pre-rift) nature of the lithosphere beneath the Ethiopian and Somalian plateaus surrounding the rift valley. We finally show how the data provided by this integrated analysis suggest that rift sectors characterized by an asymmetric architecture can directly progress to focused axial tectonomagmatic activity, without transitioning into a symmetric rifting stage, therefore challenging previous views of evolution of rifting in the East African Rift System (e.g., Hayward & Ebinger, 1996; WoldeGabriel et al., 1990). These observations have important implications for the asymmetry of continental rifts and conjugate passive margins worldwide, which has often been explained in the context of low-angle detachment faults and models involving a lithospheric-scale simple shear deformation (e.g., Wernicke, 1985).

2. Geological Setting

The MER, at the northern end of the East African Rift System, accommodates 4–6 mm/yr, N100°E oriented extension between the major Nubia and Somalia Plates (e.g., Saria et al., 2014). This rift is traditionally subdivided into three main sectors, the Southern, Central, and Northern MER (SMER, CMER, and NMER, respectively), each differing in terms of fault timing and patterns, and lithospheric characteristics (Figure 1) (e.g., Bonini et al., 2005; Corti, 2009; Hayward & Ebinger, 1996; Mohr, 1983; WoldeGabriel et al., 1990).

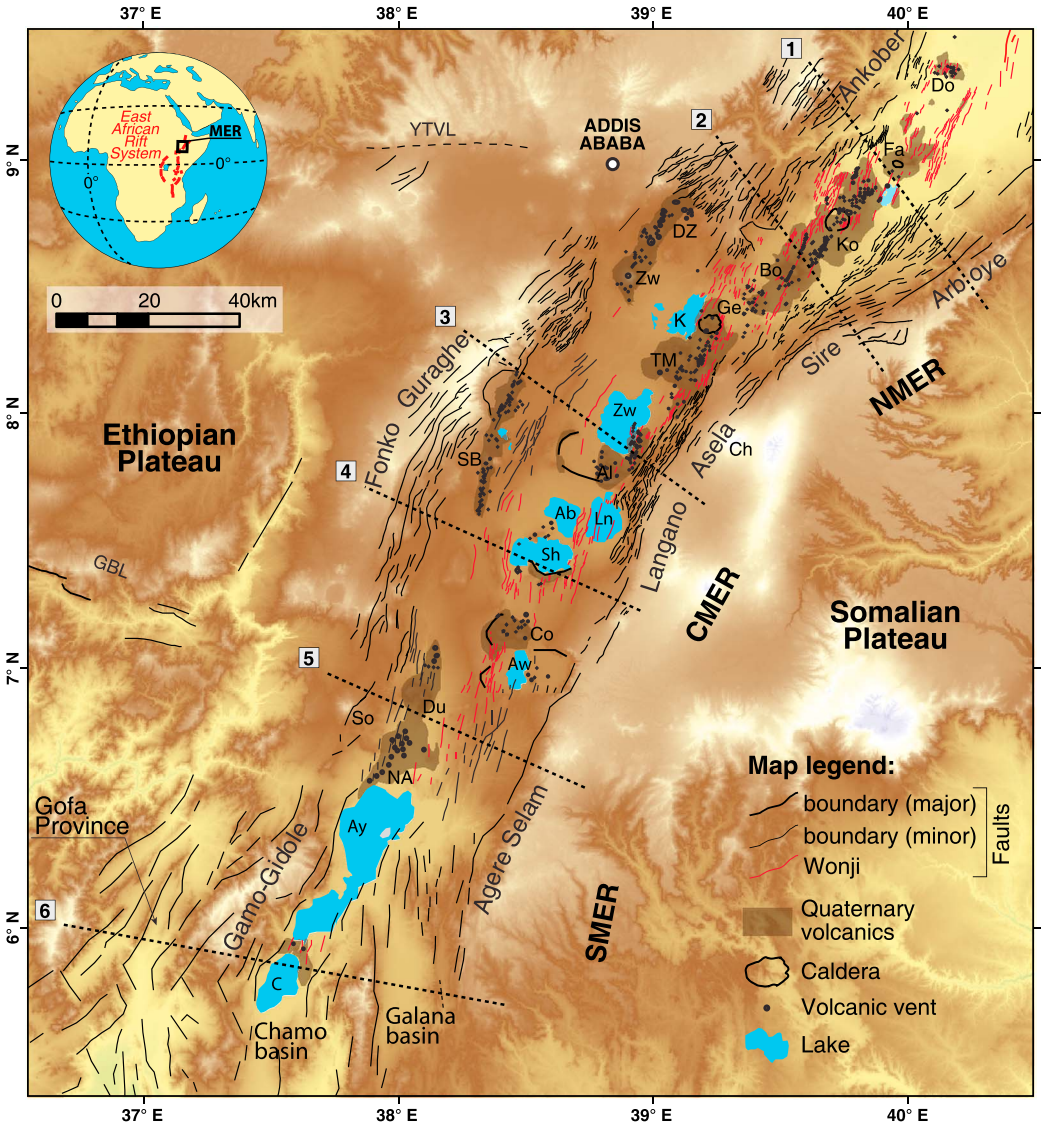

Figure 1. Fault pattern and Quaternary volcanics in the Main Ethiopian Rift (MER) superimposed on a NASA's Shuttle Radar Topography Mission (SRTM) digital elevation model. The three main rift sectors are labeled as NMER, Northern MER; CMER, Central MER; and SMER, Southern MER. The dashed lines with numbers indicate the cross sections illustrated in Figure 2. Volcanic fields and calderas are labeled as follows: Al: Aluto; Bo, Boseti; Co, Corbetti; Do, Dofan; Du, Duguna; DZ, Debre Zeyt; Fa, Fantale; Ge, Gedemsa; Ko, Kone; NA, North Abaya; SB, Silti-Butajira; TM, Tulu Moye; and Zw, Zikwala. Lakes labeled as follows: Ab, Lake Abijata; Ay, Abaya; Aw, Awasa; C, Lake Chamo; Ch: Chilalo; K, Lake Koka; Ln, Langano; Sh, Shala; Zw, Lake Ziway. Other labels: GBL: Goba-Bonga transversal lineament; So: Soddo; and YTVL: Yerer-Tullu Wellel volcano-tectonic lineament.

The MER sectors are affected by two distinct systems of normal faults: (1) the border faults and (2) a set of faults affecting the rift floor, often referred to as the Wonji Fault Belt (WFB) (e.g., Boccaletti et al., 1998; Mohr, 1962). The border faults are long (≥50 km), large-offset (typically >500 m) structures that give rise to the major escarpments separating the rift floor from the surrounding plateaus. These faults have been activated diachronously in different rift segments during the last 10–12 Ma (e.g., Balestrieri et al., 2016). Geological data and analysis of the historical and instrumental seismicity suggest that the boundary faults are largely inactive in the NMER (e.g., Casey et al., 2006; Keir et al., 2006; Wolfenden et al., 2004). Conversely, morphotectonic and geological analysis and Global Positioning System data indicate that these faults still accommodate significant extension in the CMER and SMER (Agostini, Bonini, Corti, Sani, & Manetti, 2011; Gouin, 1979; Keir et al., 2006; Kogan et al., 2012; Molin & Corti, 2015; Pizzi et al., 2006).

The WFB is an axial tectono-volcanic system characterized by relatively short (typically <20 km long), closely spaced, active faults that exhibit minor vertical throw (typically <100 m) with associated extension fractures and grabens (e.g., Acocella et al., 2003; Boccaletti et al., 1998). These faults, which are intimately associated with intense Quaternary-Recent magmatism of the rift floor, developed in the last 2 Ma (e.g., Boccaletti et al., 1998; Ebinger & Casey, 2001). The WFB is well expressed in the NMER, where its structures form clearly defined right-stepping en echelon segments obliquely cutting the rift floor (Ebinger & Casey, 2001). The abundance of Wonji faults decreases southward: these faults are in an incipient stage of development in the CMER, but practically negligible in the SMER (Figure 1) (e.g., Agostini, Bonini, Corti, Sani, & Mazzarini, 2011).

Along the MER, Quaternary-Recent volcanism is dominated by rhyolites, ignimbrites, pyroclastic deposits, and subordinate basalts (e.g., WoldeGabriel et al., 1990). In the NMER, this activity is strongly focused within the axial WFB (e.g., Ebinger & Casey, 2001). Geophysical data indicate that extension is currently accommodated via a combination of magma intrusion and normal faulting (e.g., Keir et al., 2006; Keranen et al., 2004; Mackenzie et al., 2005), with magma intrusion modifying the composition and thermal structure of the crust and lithosphere beneath the WFB (e.g., Beutel et al., 2010; Daniels et al., 2014). Magmatic modification of the crust/mantle lithosphere and Quaternary-Recent volcanism decreases southward. In the SMER, consistent with a limited volcano-tectonic activity within the rift, the albeit-sparse geophysical data indicate the absence of significant magmatic modification of the crust/lithosphere (Daly et al., 2008; Dugda et al., 2005).

Overall, these along-axis variations of the distribution and characteristics of the tectono-magmatic activity have been interpreted to reflect a transition from initial rifting in the SMER, with marginal deformation and fault-dominated rift morphology, to advanced rifting stages in the NMER, where prominent axial intrusion, dyking, and associated normal faulting testify a phase of magma-assisted rifting during the late stages of continental rifting (e.g., Kendall et al., 2005).

Geophysical studies in the MER suggest that rift location and initial evolution have been controlled by a NE-SW to N-S trending lithospheric-scale pre-existing heterogeneity (e.g., Bastow et al., 2005, 2008; Cornwell et al., 2010; Gashawbeza et al., 2004; Keranen et al., 2009; Keranen & Klemperer, 2008), which largely controlled the trend of the Cenozoic rift faulting (e.g., Kazmin et al., 1980; Mohr, 1962). This pre-existing heterogeneity corresponded to a suture zone which separated two distinct Proterozoic basement terranes beneath the Ethiopian and Somalian plateaus (e.g., Abdelsalam & Stern, 1996; Berhe, 1990; Stern, 2002; Stern et al., 1990; Vail, 1983). Extension occurred at approximately the same time as, and after, hot spot-related flood basalt volcanism (Wolfenden et al., 2004), possibly connected to the African Superplume found in the lower mantle beneath southern Africa (e.g., Ritsema et al., 1999). The reactivation of the pre-existing heterogeneity is interpreted to have occurred at the eastern edge of the upwelling mantle not above its center (e.g., Bastow et al., 2008), as documented in other flood basalt provinces (Courtillot et al., 1999) and suggested by theoretical modeling (Tommasi & Vauchez, 2001).

Several tectonic events affected Ethiopia prior to the Cenozoic rifting, from collision during the Precambrian to Mesozoic extension (Abbate et al., 2015, and references therein). This long pre-Cenozoic history of tectonic events created pre-existing heterogeneities with variable orientation that have controlled the development of the East African Rift System in Ethiopia (e.g., Korme et al., 2004). At a regional scale, for instance, large-scale E-W or WNW-ESE heterogeneities have controlled the development of major transversal volcano-tectonic lineaments, such as the Yerer-Tullu Wellel Volcanic Lineament (YTVL) and the Goba-Bonga (Figure 1), affecting the rift and the surrounding plateaus (e.g., Abebe Adhana, 2014, and references therein) and marking the transition between the different MER sectors. At a more local scale, pre-existing basement fabrics may have controlled fault and volcanic edifice geometries (e.g., Corti, 2009, and references therein).

3. Methods and Results

3.1. Structural Cross Sections in the Different MER Segments

Simplified geological profiles across different sectors of the MER are illustrated in Figure 2. In these profiles, the subsurface geology and the resulting basin architecture are derived from published cross sections, extrapolation of surface geology, or available subsurface data (see list of references in the caption of Figure 2). Faults are differentiated based on their exposed minimum vertical displacement (e.g., Laó-Dávila et al., 2015), a value that underestimates the actual fault motion since other processes (e.g., erosion and deposition)

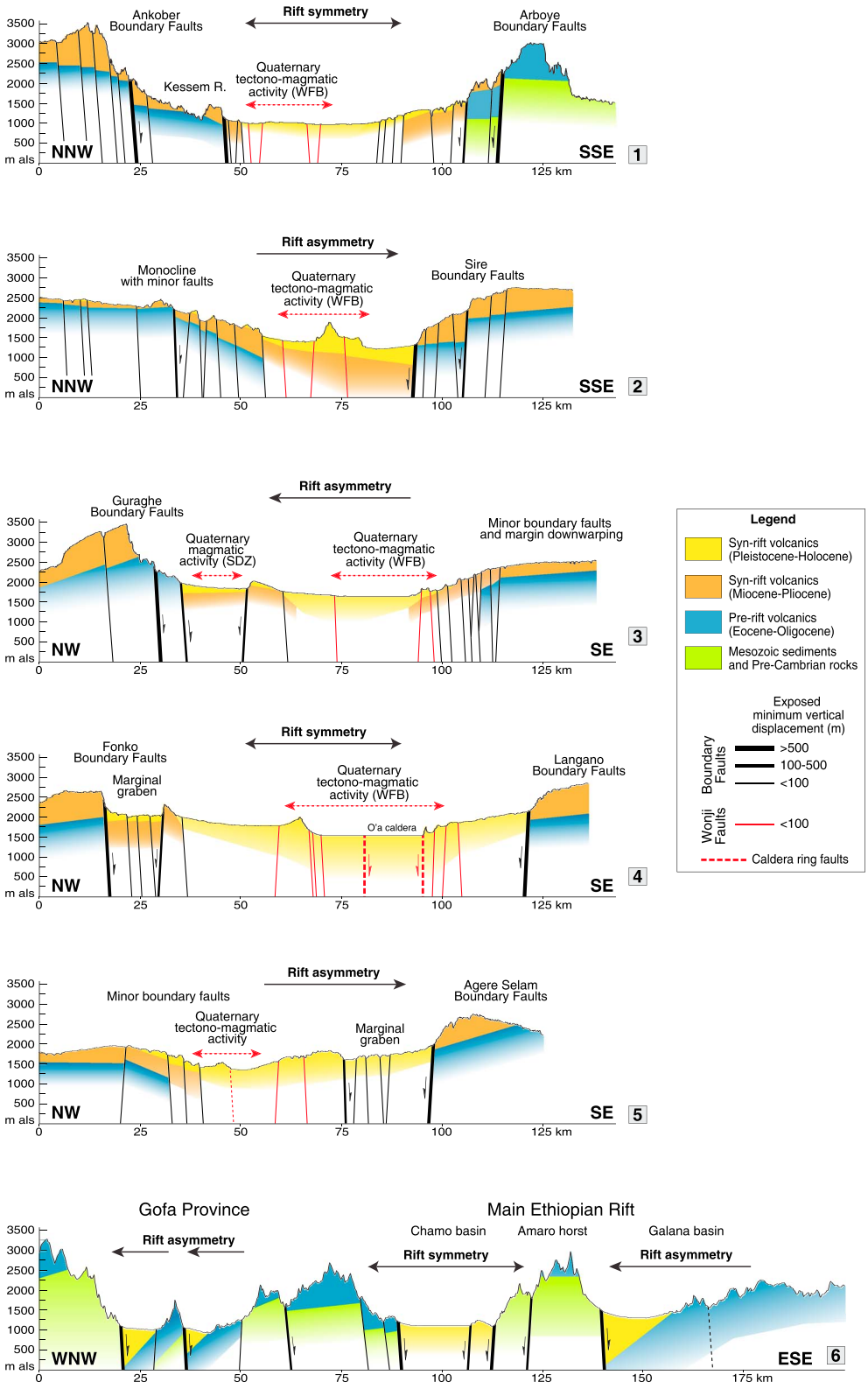

Figure 2. Simplified geological profiles across different sectors of the MER. Topographic profiles are extracted from SRTM digital elevation models, with vertical exaggeration of 10. WFB: Wonji Fault Belt; SDZ: Silti Debre Zeit volcanic belt. Sources for the geological profiles: Agostini, Bonini, Corti, Sani, and Manetti (2011); Abebe et al. (2005); Corti et al. (2013); Davidson (1983); Ebinger et al. (1993, 2000); Ethiopian Mapping Agency (1978, 1981); Ethiopian Mapping Authority (1996); Hutchison et al. (2015); Philippon et al. (2014); and Wolfenden et al. (2004).

likely altered the topography of the plateaus and the rift floor (see below). Henceforth, we use the term "rift symmetry" when the cumulative exposed minimum vertical displacement on major boundary faults is similar on both rift margins, and the term "rift asymmetry" when this value is significantly lower on one margin with respect to the other (e.g., Laó-Dávila et al., 2015). This classification is supported by basin architecture derived from the above mentioned analysis.

1. Profile 1 crosses the northern portion of the NMER and shows an approximately symmetric rift structure, with major boundary fault systems on both western and eastern margins (Ankober and Arboye, respectively; Figure 1); the recent tectono-magmatic activity of the WFB is well developed at the rift axis in this area (Fantale-Dofan magmatic segment; e.g., Ebinger & Casey, 2001). The boundary faults are generally interpreted to have been deactivated during the Pleistocene (Casey et al., 2006; Wolfenden et al., 2004), although the high levels of seismicity recorded in the period of 2002–2003 indicates ongoing fault slip along the Ankober border fault system (Keir et al., 2006). However, most active tectonics in the area is believed to be accommodated via a combination of intrusion, dyking, and normal faulting within the WFB (Keir et al., 2006). This portion of the rift passes into a more asymmetric rift structure northward into Afar, with a major escarpment on the western side (Ankober fault system; e.g., Wolfenden et al., 2004).
2. Similarly, the southern portion of the NMER (Profile 2) displays a marked asymmetry, with the large offset main boundary fault system on the eastern side (Sire fault system) and the northwestern margin characterized by a faulted flexure (e.g., Wolfenden et al., 2004). The axial portion of the rift is affected by recent tectonic and magmatic activity associated with the WFB (Boseti magmatic segment), which accommodates the largest portion of current plate motion (e.g., Kogan et al., 2012).
3. Profile 3 illustrates the across-axis structure of the northern portion of the CMER, which is characterized by a major boundary fault system on the western margin forming the Guraghe escarpment. The opposite side of the rift is marked by the Asela-Sire fault system, whose morphological expression may be at least in part obscured by the prominent Pliocene-Quaternary volcanism of large volcanoes (such as Chilalo) at the rift margin (Figure 1) (e.g., Boccaletti et al., 1999). A general tilting of eastern margin toward the rift axis is observed (e.g., Agostini, Bonini, Corti, Sani, & Manetti, 2011; Pizzi et al., 2006); although this tilting may be locally controlled by loading from magma intrusion (Corti et al., 2015), the margin architecture may support a rift asymmetry with master fault on the western side. The recent tectono-magmatic activity is well developed on the WFB close to the Asela margin, east of Lake Ziway; Quaternary-Recent magmatic activity also characterized the western margin on the Silti Debre Zeit alignment, although not associated with surface faulting (e.g., Agostini, Bonini, Corti, Sani, & Manetti, 2011). Both the boundary fault systems and the WFB accommodate the recent-current deformation in the area (e.g., Agostini, Bonini, Corti, Sani, & Manetti, 2011; Keir et al., 2006; Molin & Corti, 2015; Pizzi et al., 2006).
4. Further south, the CMER (Profile 4) presents well-expressed, large boundary faults at Fonko and Langano (e.g., Agostini, Bonini, Corti, Sani, & Manetti, 2011), which give rise to a roughly symmetric architecture. The WFB volcano-tectonic activity is developed close to the rift axis, and well expressed by the O'a caldera, now occupied by Lake Shala. Both the rift margins and the WFB are active in this rift sector and accommodate the recent-current deformation in the area (e.g., Agostini, Bonini, Corti, Sani, & Manetti, 2011; Keir et al., 2006; Molin & Corti, 2015).
5. Profile 5 illustrates the SMER north of Lake Abaya, which is an asymmetric structure characterized by a major fault escarpment on the eastern side (Agere Selam escarpment) and a faulted, riftward dipping monocline at the Soddo margin on the western side (e.g., Corti et al., 2013; Philippon et al., 2014). This latter margin is affected by numerous, closely spaced, small normal faults with associated widespread Pleistocene-Holocene volcanism (Figure 1). The architecture of faults and the distribution of volcanic vents resemble the tectono-magmatic architecture of the WFB, but magma geochemistry is akin to that of the Silti Debre Zeit volcanic belt. Overall, the current volcano-tectonic activity in the north Abaya region is mostly accommodated at the western margin of the rift; conversely, there is little evidence for significant current tectonic activity on the eastern margin (Corti et al., 2013; Kogan et al., 2012; Philippon et al., 2014; Rooney, 2010).
6. Further south (Profile 6) rifting becomes more complex: deformation affects a much wider region and is partitioned between the SMER and the Gofa Basin and Range or Gofa Province (e.g., Ebinger et al., 2000; Philippon et al., 2014, and references therein). The SMER itself is subdivided in two different basins, Chamo and Galana, separated by a prominent basement horst (Amaro Horst). The Galana basin displays a

marked asymmetry with a major boundary fault system on the western side, whereas the Chamo basin is more symmetric (Ebinger et al., 1993). The minor basins composing the Gofa Province are generally asymmetric, with a master fault on the western sides (e.g., Ebinger et al., 2000). Recent volcanism is almost absent in these basins, and the current tectonic activity is likely accommodated by large boundary faults of both the SMER (e.g., Kogan et al., 2012; Philippon et al., 2014) and the Gofa Province (e.g., Ebinger et al., 2000; Philippon et al., 2014).

Overall, analysis of these data indicates that the MER displays significant along-axis variations in structure and can be subdivided in different portions characterized by symmetric or asymmetric structure.

3.2. Topography and Hydrography Patterns

We conduct quantitative analysis of topography and hydrography patterns as an independent test of rift symmetry. The flexural uplift generates topography and, as a consequence, rivers incise, further unloading the footwall and enhancing its isostatic uplift (Tucker & Slingerland, 1994). This positive feedback should increase the possible asymmetry of the rift structure. The role of erosion in shaping topography is considered of first-order importance since surface processes exert a control on regional-scale phenomena (Tucker & Slingerland, 1994, and references therein), and has been widely explored in orogenic belts (Brocklehurst & Whipple, 2002; Burbank, 2002; Champagnac et al., 2009; Molnar & England, 1990; Stern et al., 2005; Willett, 1999; Willett et al., 2001; Wittmann et al., 2007, and references therein) and passive margins (Anell et al., 2009; Kooi & Beaumont, 1994; Pazzaglia & Gardner, 1994; Tucker & Slingerland, 1994). However, little progress has been made to understand such dynamics in the context of extensional tectonics. The works available concentrate mainly on the mechanical unloading due to extension (Müller et al., 2005; Petit et al., 2007; Poulimenos & Doutsos, 1997; Stern & ten Brink, 1989; Weissel & Karner, 1989; Weissel, Malinverno, & Harding, 1995) or on the interaction between surface and large-scale lithosphere processes (Burov & Cloetingh, 1997; Daradich et al., 2003; Huismans & Beaumont, 2005; Mueller et al., 2009; Pik et al., 2008).

In the following sections, we analyze the topography and hydrography of the MER to place fully independent constraints on the symmetry of the rift and to characterize the major surface processes and to investigate the possible role of erosion in rift architecture and its along-axis variations (Figure 3). We use NASA's Shuttle Radar Topography Mission (SRTM) digital elevation models, whose ~90 m resolution is suitable for regional analysis.

3.2.1. Swath Profiles

To describe and quantify the general topographic trend of the MER and surroundings, we generate six swath profiles coincident with the structural profiles (Figures 1 and 3). They show the trend of maximum, minimum, and mean elevation in a single plot (Isacks, 1992; Molin, Pazzaglia, & Dramis, 2004; Ponza et al., 2010). We extract them from the SRTM digital elevation models in GIS environment, sampling topography every 2 km into observation windows 30 km wide. The length of each profile is chosen to represent the MER, as in the structural profiles, but also the surroundings to better show the possible river response to tectonic input. In the swath profiles, in correspondence with each rift margin, we measured the drop in elevation from the highlands to the rift floor and the relative topographic gradient. Since the rift floor is blanketed by volcanic edifices and deposits, the measurements consider just the topographic expression of the interaction between tectonics, volcanism, and surface processes.

Swath profile 1 extends from the Ethiopian Plateau in the NNW to the Somalian Plateau in the SSE (Figures 3 and 4). In the NNW, the trend of mean topography shows the flexural uplift affecting the rift shoulder (2.5–3 km of elevation), as documented by Weissel et al. (1995) and Sembroni, Faccenna, et al. (2016). A similar flexural strain is possibly hidden by the strong fluvial erosion affecting the SSE sector where the Somalian Plateau is limited to a narrow strip of land with a mean elevation of ~2,700 m (Figures 3 and 4). The MER appears symmetric, limited on both sides by escarpments with similar height and topographic gradient (Table 1). Profile 1 shows also a large difference (~1,000 m) in maximum and minimum topography along the northwestern rift shoulder, indicating high local relief. Molin and Corti (2015) interpreted this as typical of a mature stage of rifting when rift margins are highly incised by a well-organized fluvial network composed by concave and steep rivers.

Swath profile 2 is located immediately to the east of Addis Ababa where the roughly E-W trending transverse structures, namely, the YTVL (Abebe et al., 1998), separates the NMER and CMER. This profile shows the rift as an asymmetric structure (Figure 4) confirmed also by the large difference in topographic gradient between

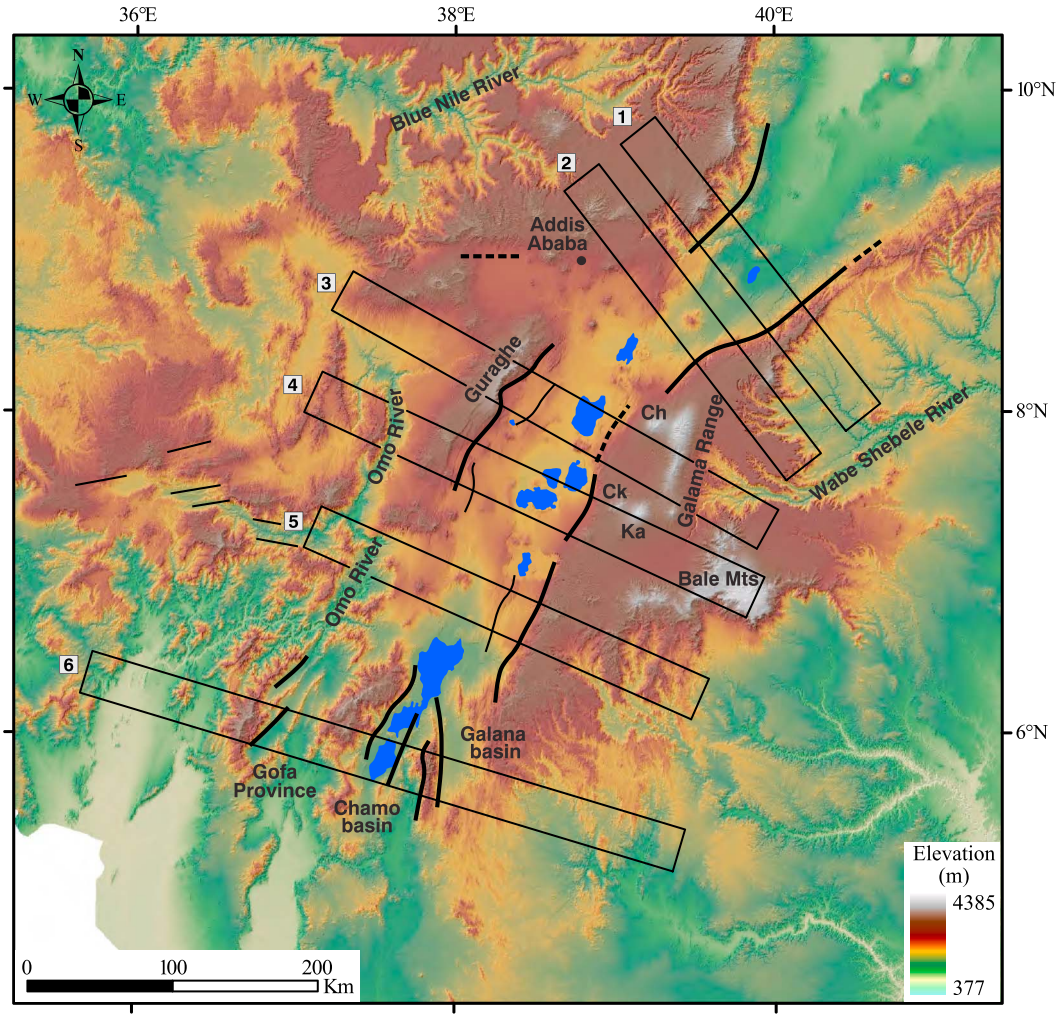

Figure 3. Topography of the study area (SRTM digital elevation model, 90 m of resolution) including the main tectonic structures (solid and dashed lines) and the swath profiles location. Ch: Mt Chilalo; Ck: Mt Chilke; Ka: Mt Kaka.

the western and eastern margins (Table 1): the mean elevation of the Ethiopian Plateau decreases progressively from ~3,000 m to <1,500 m towards the rift floor in a distance of ~60 km; conversely, the Somalian Plateau is well defined with a maximum almost flat topography attained at 2,500 m. Here the difference in elevation of about 1,000 m between maximum and minimum topography evidences a strong incision of the inner portion of the Somalian Plateau. This strongly contrasts with the Ethiopian Plateau, where incision is <500 m.

Swath profile 3 in the CMER shows, on both Ethiopian and Somalian plateaus, a large difference between maximum and minimum topography, i.e., a local relief of ~1,000 m. West of the CMER, the Ethiopian Plateau is eroded by the tributaries of the Omo River so that its westernmost portion appears to be separated from the Guraghe structure. East of the CMER, the highlands are poorly eroded except where the valley of the Wabe River is located (Figure 3). The MER shows an asymmetrical configuration with the Guraghe steep escarpment on the northwestern side (~1,500 m in height) and a step-like scarp on the southeastern side where the highest peak corresponds to the Galama Volcanic Range. Such configuration is well described by the differences in rift margin elevation drop and topographic gradient values, being the western margin characterized by much higher values than the eastern one (Table 1).

In Swath profile 4 (southern portion of the CMER; Figures 3 and 4) the mean topography is slightly above 2,000 m west of the Omo River valley but increases (to >2,500 m) toward the rift margin. Similarly, the Somalian Plateau is ~2,500 m except where volcanoes (Mt Chilke, Mt Kaka, and Bale Mts) rise from it. Here

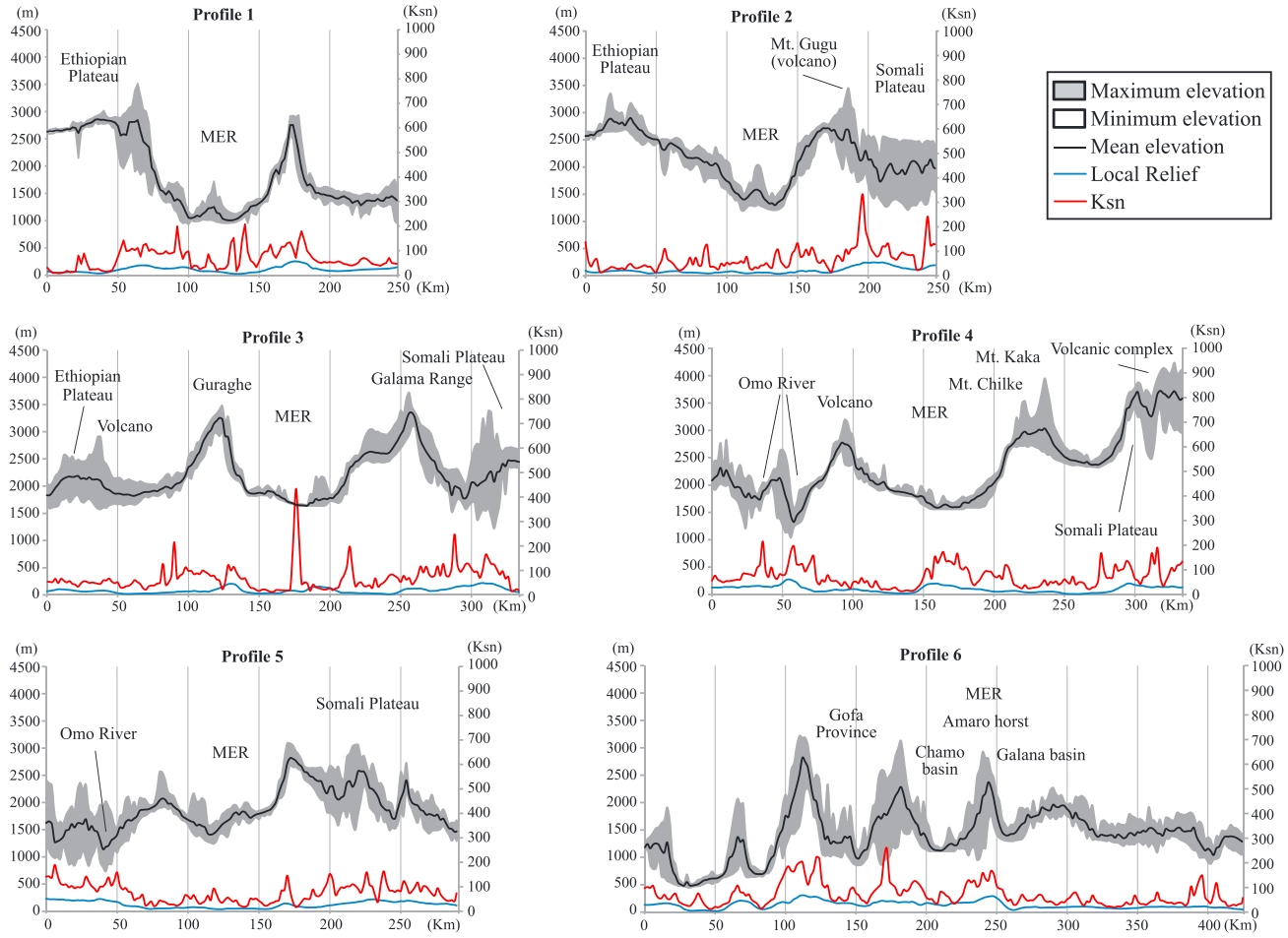

Figure 4. Swath profiles illustrating the maximum, mean, and minimum elevation pattern cutting across the MER. The plots include also the variation in the mean values of local relief and channel steepness index (see text for explanation and Figure 5 for profile location).

Table 1
Summary of the Characteristics of the Different MER Sectors (See Text for Further Details)

Sector	Length (km)	Structure	Main border fault	Active deformation	Magmatic activity	Rift margin elevation drop (m)		Topography gradient of rift margin	
						West	East	West	East
1	70	Symmetric	-	Mostly axial (minor activity in the Western margin)	Axial (Wonji)	1,799	1,750	0.047	0.040
2	100	Asymmetric	East	Axial	Axial (Wonji)	1,500	1,416	0.019	0.042
3	50	Asymmetric	West	Marginal	Marginal (Wonji + SDZ)	1,392	870	0.058	0.029
4	60	Symmetric	-	Mostly marginal (axial subordinate)	Axial (WFB)	946	897	0.019	0.027
5	100	Asymmetric	East	Marginal (activity at the Western margin)	Marginal (mixed Wonji + SDZ characteristics)	665	948	0.019	0.067
6	120	Symmetric (Chamo basin) Asymmetric (Galana basin, Gofa Province)	East and West	Mostly marginal (axial subordinate)	Almost absent	1,165 (Chamo basin)	1,248 (Chamo basin)	0.042 (Chamo basin)	0.037 (Chamo basin)

the MER presents a nearly symmetrical shape with escarpments ~1,000 m high characterized by a similar elevation drop (~900 m on average; Table 1). Such a trend is not confirmed by the topography gradient, which is slightly higher in the eastern margin (Table 1). Such discrepancy is related to the different distribution of extension-related deformation on the two margins. Whereas the eastern margin is characterized by a single major fault at the base of the Langano escarpment, the western margin is marked by several normal faults (including the major Fonko Fault and associated synthetic and antithetic subparallel structures) distributed over a wider deformation domain (Figures 1 and 2) (Agostini, Bonini, Corti, Sani, & Manetti, 2011; Molin & Corti, 2015).

Swath profile 5 is just south of the boundary between the CMER and SMER, where the E-W Goba-Bonga lineament (Abbate & Sagri, 1980) is located. Here the Ethiopian Plateau is characterized by low elevation (~2,000 m) and is deeply incised by the Omo River. At the rift margin, topography decreases progressively toward the rift floor (1,500 m). The MER appears to be asymmetric to the east, where the margin shows an elevation drop of ~950 m and a topography gradient of 0.067 (Table 1); mean topography increases to >2,500 m (Somalian Plateau) and then decreases progressively. Here the Somalian Plateau is strongly incised by the fluvial network. To the west, the rift margin presents a small elevation drop (665 m) and topography gradient (0.019; Table 1); in this portion there is no morphological evidence of a tectonic escarpment (Figure 3).

Swath profile 6, across the southernmost portion of the dome-shaped topography, cuts across the complex region of diffuse deformation including the SMER and the Gofa Province (see above). The profile reveals the presence of several tectonic basins mostly west of the MER. Here the MER (corresponding with the Chamo basin) is narrower and symmetrical with both margins standing at a mean elevation of more than 2,000 m and presenting similar elevation drop and topography gradient values (Table 1). The topography becomes relatively regular on the southeastern portion (~1,500 m in mean elevation) where the profile crosses the Precambrian rocks standing at the periphery of the dome-shaped topography relative to the upwelling of the Afar plume (Sembroni, Faccenna, et al., 2016; Sembroni, Molin, et al., 2016, and references therein).

3.2.2. Local Relief

We constrain a map of local relief of the study area to quantify the difference in elevation between valley bottoms and peaks, and to investigate the spatial distribution of river incision. In detail, we smooth the maximum and minimum topography of the SRTM digital elevation models by a 10 km diameter circular moving window (low-pass filter) in GIS environment. We choose such a value since it is the average spacing of the main valleys (seventh Strahler order with respect to a critical drainage area of ~4 km^2). This allows the removal of small valleys, highlighting the regional-scale features. The results of the smoothing are two surfaces: the subenvelope surface, which describes the general pattern of valley bottoms elevations, and the envelope surface, which connects peak elevations. We obtain the local relief map by arithmetically subtracting the resulting surfaces (Figure 5a). To demonstrate better the relationship between topography and river incision, we extract six swath profiles across the local relief map. In more detail, using the same observation windows of Figure 3, we sample the local relief along five profiles and calculate the mean local relief value. The results are plotted in Figure 4 to facilitate the comparison between the trend of local relief and the topography configuration.

The study area is characterized by a general low local relief (<300 m) with the lowest values concentrated in the MER and the portions of the Ethiopian and Somalian plateaus preserved by erosion (Figure 5a). Such features represent the ancient top surface of the Trap deposits and have been used by some authors to calculate the volume and thickness of flood basalts (Gani, Abdelsalam, & Gani, 2007; Sembroni, Faccenna, et al., 2016) and to reconstruct the post-Trap topography (Sembroni, Faccenna, et al., 2016). Values >300 m are in the MER where volcanoes and active tectonics cause the increase of local relief up to 600 m (Figures 4 and 5a). Values >300 m characterize also the inner sectors of the Ethiopian and Somalian plateaus, where rivers incised deep canyons, and the rift margins (Figures 4 and 5a). Here the relief increases where the extensional tectonics generates escarpments and possibly a flexural uplift of the footwall (Sembroni, Faccenna, et al., 2016). Indeed, relatively high values of local relief are at the footwall of the major border faults, further evidence for the symmetric or asymmetric structure of the rift (Figures 4 and 5a).

The topography configuration is much more complicated in the southernmost sector of the MER where several tectonic basins as well as the strong incision of the Omo River make difficult the reading of the local relief map (Figures 4 and 5a).

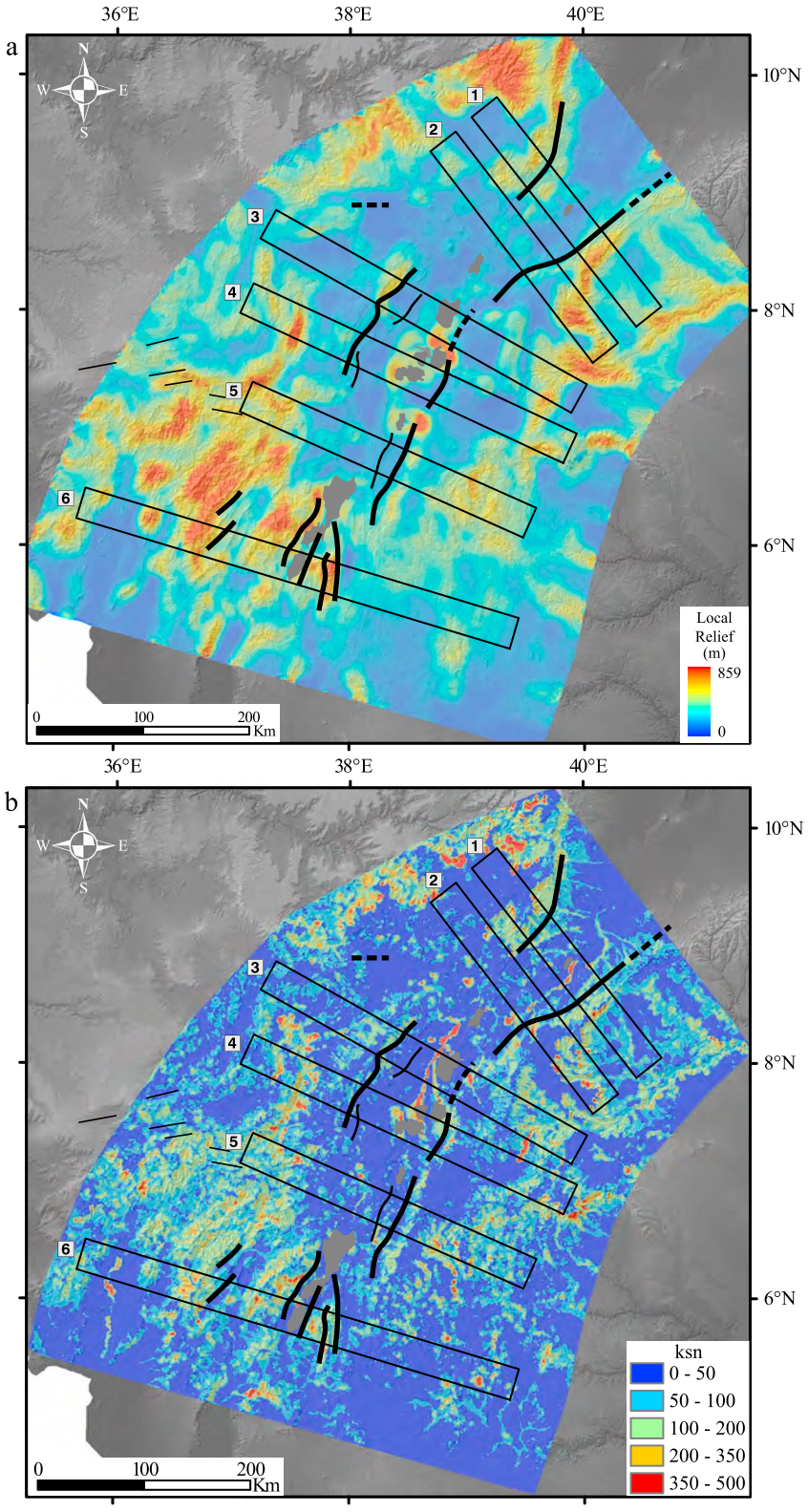

Figure 5. (a) Map of the local relief of the study area: Note how the correspondence between high values of local relief at the rift margins and location of the main structures evidences the symmetry/asymmetry of the MER sectors. (b) Map of the along-channel variation of the steepness index: along the rift margins high values of channel steepness correspond with the main tectonic structures.

3.2.3. k_{sn} Map

Since hydrography is sensitive to local and regional tectonic inputs (e.g., Lock et al., 2006; Molin & Corti, 2015; Pazzaglia, Gardner, & Merritts, 1998; Sembroni, Molin, et al., 2016; Scotti et al., 2013; Tomkin et al., 2003; Wegmann & Pazzaglia, 2002; Wobus et al., 2006), we investigate the MER drainage system focusing on the channel steepness variation.

To study river incision both at steady and transient state, a power law is widely used which relates channel slope S and drainage area A (Flint, 1974; Hack, 1957; Howard et al., 1994; Kobor & Roering, 2004; Schorghofer & Rothman, 2002; Sklar & Dietrich, 1998; Snyder et al., 2000; Whipple, Hancock, & Anderson, 2000; Whipple & Tucker, 1999):

$$S = k_s A^{-\theta}, \quad (1)$$

where k_s and θ are the steepness and concavity indices. Several studies evidence a positive correlation between steepness index and uplift rate, although it is strongly influenced by geologic setting and climate (e.g., Kirby & Whipple, 2001; Kirby et al., 2007; Molin & Corti, 2015; Snyder et al., 2000; Whipple, 2004; Wobus et al., 2006). Under steady state conditions, θ = 0.4–0.6, but theoretically ~0.45 (Kirby & Whipple, 2001; Snyder et al., 2000; Tarboton et al., 1989; Whipple, 2004; Whipple & Tucker, 1999; Whipple et al., 2007). This theoretical value is used as a reference concavity to normalize the steepness index (k_{sn}; Wobus et al., 2006). This allows the comparison of rivers regardless the size of the drainage basins. To reveal the general variation in steepness index values along river courses, we extract the map of the along channel variation in k_{sn} by using the Stream Profiler tool developed by Whipple et al. (2007); the critical drainage area is set at 10^7 m^2 to obtain a detailed analysis of the river network up to the third Strahler order. Once obtained, the linear shape file has been converted into a point shape file and interpolated by a nearest neighbor triangulation algorithm to extract the areal distribution of k_{sn}.

To show the pattern of k_{sn} with respect to topography, we extract six swath profiles across the k_{sn} map. Using the same observation windows as Figure 3, we sample the k_{sn} map along five profiles and calculate the mean value. The results are plotted in Figure 4 to compare the channel steepness trend with the topography pattern. Since the channel steepness is very sensitive also to very small variation in slope, both map and profiles show abrupt changes in values on short distance.

The k_{sn} map (Figure 5b) shows a correspondence between high values of k_{sn} (>350, which coincide with knickpoints and knickzones) and rock type changes, especially along the Ethiopian and Somalian plateaus scarps. Medium-high values (>200) correspond to the rift margins (Figures 4 and 5b) where the tectonic structures have generated knickpoints and knickzones (Molin & Corti, 2015). At the footwall of the major border faults of MER, higher values of k_{sn} evidence the symmetric or asymmetric structure of the rift (Figures 4 and 5b).

4. Discussion

We have used structural, topographic, and hydrographic analyses to constrain the architecture and segmentation of the MER, considering the interaction between tectonics and fluvial erosion and the role of such interaction in dictating the evolution of the rift.

The MER displays significant along-axis structural variation: the MER's three traditional subdivisions, the NMER, CMER, and SMER (e.g., Agostini, Bonini, Corti, Sani, & Mazzarini, 2011), can be further subdivided into portions characterized by symmetric or asymmetric structure (Figure 6a and Table 1). In general, ~70% of the 500 km long rift is asymmetric. The symmetry or asymmetry of the rift is reflected in the topography and in the rift margin elevation drop and topography gradient. The tectonic symmetry/asymmetry is supported by the convergence/divergence of such values for both rift margins (Table 1). Where major boundary faults are present, the rift margin reaches higher elevations (Figures 2–4), locally showing a decrease at the footwall of the tectonic structures typical of flexural uplift (Sembroni, Molin, et al., 2016). This process increases elevation and therefore stream power and channel steepness (Figure 5b) that results in river incision (Figure 5a). Unloading related to fluvial erosion could have enhanced the flexural uplift, generating a positive feedback between tectonics and surface processes. This dynamic coupling between flexural uplift and fluvial incision probably amplified the symmetric or asymmetric structure of the rift. A similar scarp evolutionary scenario has been predicted by numerical modeling (Kooi & Beaumont, 1994; Petit et al., 2007; Tucker & Slingerland, 1994).

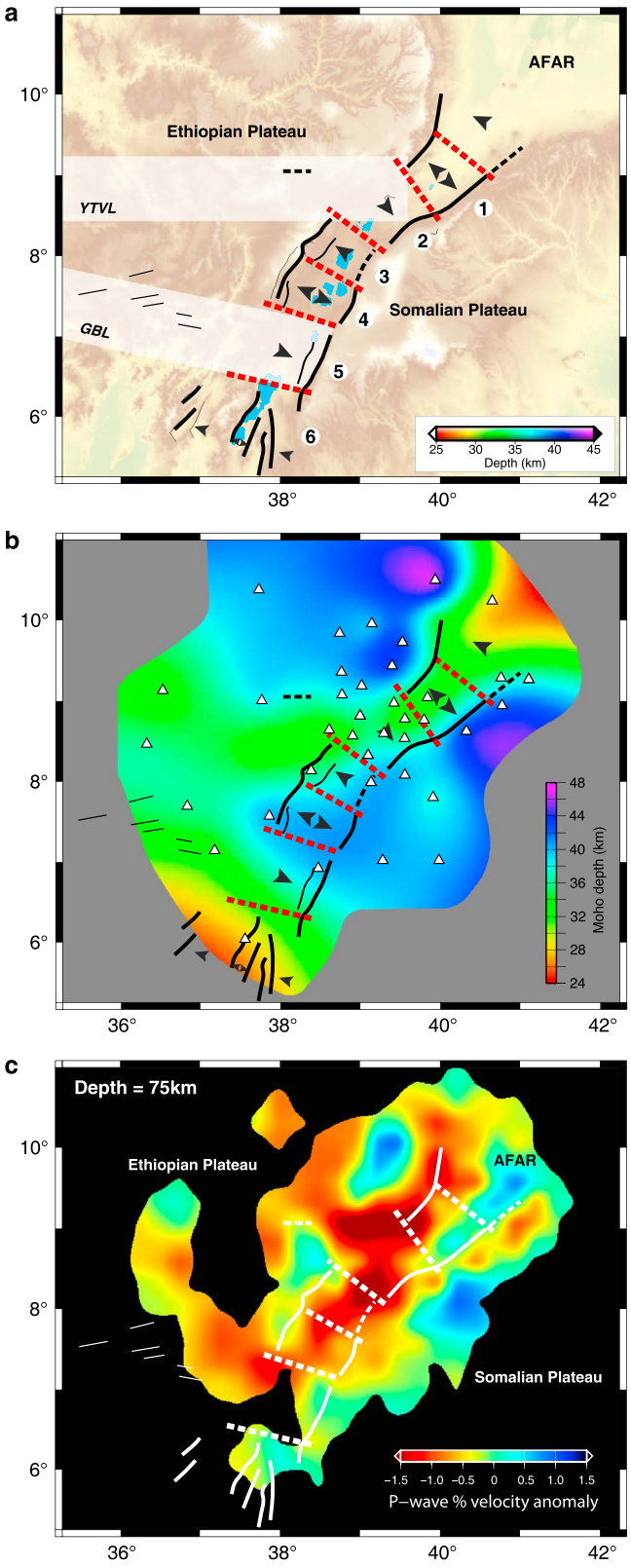

Figure 6. (a) Interpreted along-axis variations in the structure of the Main Ethiopian Rift. The single arrows indicate the polarity of the different rift sectors; the double arrows indicate symmetry of rifting. The whitish boxes indicate the hypothesized extent of the transversal: Yerer-Tullu Wellel (YTWLYTVL) and Goba-Bonga (GBL) volcano-tectonic lineaments. (b) Contour map of Moho depth in the MER (after Keranen et al., 2009). (c) Depth slices through the *P* wave velocity model of Bastow et al. (2008) at 75 km depth. See text for further details.

Generally, most of the asymmetric sectors have a master fault system located on the eastern margin. In particular, >70% of the eastern margin is marked by a major boundary fault; the remainder is marked by minor faulting and monoclines. In some cases (e.g., Asela), the margin morphology is masked by prominent recent volcanism, and therefore, 70% can be considered a lower bound. Next, we interpret the spatial pattern of border faulting in light of geophysical constraints on lithospheric structure and strength.

4.1. Relations Between Rift Architecture and Pre-rift Lithospheric Rheology

The MER has developed within a region that has experienced several tectonic events, from different phases of collision during the Precambrian to Mesozoic extension (e.g., Chorowicz, 2005), which have resulted in significant lateral variations in the rheological structure of the lithosphere. The rift valley formed within an ancient suture zone sandwiched between two distinct lithospheric domains beneath the Ethiopian and Somalian plateaus (e.g., Bastow et al., 2008; Berhe, 1990; Cornwell et al., 2010; Keranen & Klemperer, 2008; Kazmin, Shifferaw, & Balcha, 1978; Vail, 1983; see above section 2). Rift architecture and the along-axis structural variations are likely controlled by differences in the crustal/lithospheric structures of these two domains.

Specifically, the eastern margin is characterized by limited along-axis variations in architecture, being dominated by large boundary escarpments along almost its entire length; this likely reflects the strong and homogeneous nature of the lithosphere beneath the Somalian Plateau (e.g., Keranen & Klemperer, 2008). Conversely, the western margin is more irregular, with segments characterized by large boundary faults (Ankober, Fonko-Guraghe, Gamo-Gidole) alternating with segments marked by gentle flexures toward the rift axis. This reflects a more complex structure of the Ethiopian plateau lithosphere, interpreted to comprise two different portions: a strong northern portion, strengthened by cooled (pre-rift) mafic underplate, and a southern portion, with thinner crust and weaker rheology (Figure 6b) (e.g., Keranen & Klemperer, 2008). This southern portion is marked by the presence of two major transversal lineaments, YTVL and Goba Bonga, resulting from the Cenozoic reactivation of pre-existing Neoproterozoic weaknesses, subparallel to the trend of the Gulf of Aden (e.g., Abbate & Sagri, 1980; Abebe Adhana, 2014; Abebe et al., 1998; Korme et al., 2004). Where these pre-existing weak heterogeneities intersect at a high angle the rift, the western margin lacks major boundary faults, which are instead replaced by gentle monoclines; this, together with well-developed faults on the eastern side, results in an overall asymmetry of the rift (Figure 6).

Geophysical analysis of the crust and mantle beneath both plateaus (e.g., Bastow et al., 2008; Dugda et al., 2005; Keranen et al., 2009; Mackenzie et al., 2005; Maguire et al., 2006; Stuart et al., 2006; Whaler & Hautot, 2006) supports this interpretation (Figure 6). Crustal thickness and bulk crustal V_p/V_s ratios are relatively heterogeneous beneath the Ethiopian Plateau (41–43 km in the NW, <40 km in the SW) compared to the homogenous crust (38–40 km thickness, 1.8 V_p/V_s ratio) beneath the Somalian Plateau (Figure 6b) (Stuart et al., 2006; Keranen et al., 2009). The crust beneath the YTVL of the Ethiopian Plateau is characterized by anomalously high V_p/V_s (1.9–2; e.g., Stuart et al., 2006), which is interpreted as evidence for the presence of melt in the crust. In support of the interpretation of elevated fluid content in the crust beneath the YTVL, magnetotelluric data show low resistivities (~2 Ωm), in contrast to the high resistivities (~100 Ωm) found beneath the Somalian Plateau. Analysis of crustal thickness indicates that the YTVL corresponds to a sharp gradient in Moho depth (Figure 6b). In particular, this transversal lineament corresponds to the boundary of the strong and thick crust of the northern portion of the Ethiopian Plateau (Keranen & Klemperer, 2008). South of the YTVL, the Ethiopian Plateau (including the Goba Bonga region) has a crust that is significantly thinner than the average crustal thickness of the Ethiopian-Somalian plateaus (see also Keranen et al., 2009). Notably, along-axis variations in crustal thickness in the Ethiopian Plateau match well the subdivision in symmetric or asymmetric rift portions we suggest, with major rift escarpments corresponding to portions characterized by thick (and likely strong) crust (Figure 6b).

Our interpretation of heterogeneous crustal composition, thickness, and strength for the Ethiopian Plateau is supported by geophysical constraints on properties of the whole plate. The 75 km depth slice through relative arrival-time body wave tomographic model of Bastow et al. (2008) shows distinctive low-velocity anomalies that extend from the rift valley to the Ethiopian Plateau in two lobes specifically beneath the YTVL and Goba Bonga transversal lineament (Figure 6b). These low-velocity anomalies are best explained by a combination of a thermal anomaly and partial melting in response to upwelling and decompression of the asthenosphere caused by localized extension and thinning of the lithosphere beneath the two

volcanic lineaments (e.g., Bastow et al., 2010; Gallacher et al., 2016). In support of the hypothesis of plate weakening, the values of the effective elastic plate thickness (T_e; Pérez-Gussinyé et al., 2009) are generally much lower and more heterogeneous for the Ethiopian Plateau than for the Somalian Plateau, where T_e can reach values >60 km. The most prominent asymmetries occur south of Addis Ababa where the Ethiopian Plateau is marked by major E-W trending YTVL and the Bonga Goba transversal lineaments. This latter lineament corresponds to a narrow E-W domain where T_e decreases to 10–15 km (Pérez-Gussinyé et al., 2009). Whether zones of thinned crust, and inferred thinned lithosphere, beneath the YTVL and the Bonga Goba transversal lineament are directly caused by pre-rift lithospheric thin zones or by synrift extension that exploits pre-rift zones of weakness is impossible to tell. However, both interpretations strongly suggest that pre-rift structural control exerts a significant influence on the current structure of the lithosphere.

In summary, all the above mentioned observations suggest that although different processes may have contributed to the present architecture of the MER (e.g., flexure during initial rifting stages, Kazmin et al., 1980, and bending related to magma intrusion, Corti et al., 2015; Buck, 2017), the major control has been likely exerted by the different rheological nature of the Ethiopian and Somalian plateaus. This supports recent observations from other continental rifts (e.g., Malawi Rift and Upper Rhine Graben) illustrating that along-axis variations in basement fabric have a strong influence on basin architecture and segmentation as well as on the characteristics of the rift margins (e.g., Grimmer et al., 2017; Laó-Dávila et al., 2015).

4.2. General Implications for Continental Rifting and Break-up

Overall, our integrated analysis suggests that the MER is characterized by a Mio-Pliocene rift segmentation controlled by the pre rift lithospheric structure, which results in 80–100 km rift portions characterized by alternating symmetric/asymmetric basins. The timescale (~10 Myr) of the formation of this architecture is at least partially due to the positive feedback between tectonic and fluvial erosion, which emphasizes the flexural uplift of the rift margin faults and its topographic expression. With increasing extension into the Quaternary, the along-rift segmentation of the axis is progressively defined by the 40–60 km long magmatic segments in the NMER (Ebinger & Casey, 2001). This indicates that whereas rift architecture is mostly controlled by the pre-rift lithospheric structure during initial rifting stages, other processes (such as magmatism and rift obliquity; e.g., Corti, 2008; Ebinger & Casey, 2001) define axial segmentation during more advanced rifting (e.g., Ebinger, 2005).

One important outcome of our work is that there is no evidence for a progressive evolution from asymmetric to symmetric rifting with time, as proposed by previous works (Hayward & Ebinger, 1996; WoldeGabriel et al., 1990). Indeed, asymmetric rifts may be characterized by a direct focusing of the tectonic-magmatic activity at the rift axis, as observed in the NMER (see section 2 in Figure 2; Ebinger, 2005; Ebinger & Casey, 2001) and supported by modeling of rift evolution (e.g., Corti, 2008). An alternative behavior has been observed in the northern portion of the SMER, where deformation seems to have transitioned from an asymmetric structure with master fault on the eastern side to localized volcano-tectonic activity at the western margin in the Soddo area (Corti et al., 2013), a process which may have been controlled by localized magma intrusion and a consequent local weakening of the crust/lithosphere.

Such observations have important implications for the asymmetry of conjugate passive margins worldwide. Our data suggest that asymmetry may result from the pre-rift asymmetric nature of the lithosphere, which controls the development of major boundary faults on one side, and controls the less-developed faulting on the opposite side. The influence of the rheological and geometrical characteristics of lithosphere on the asymmetry of a rift system has been evidenced also by numerical models (e.g., Huismans & Beaumont, 2014) indicating that a strong lithosphere supports large flexural stresses that control the flank uplift and, consequently, the erosion rate. Therefore, asymmetry does not require low-angle detachment faults and lithospheric-scale simple shear deformation (e.g., Wernicke, 1985): our data support the high-angle nature of large boundary faults (e.g., Keir et al., 2006), arguing against significant simple shear deformation. The topographic expression of these structures is enhanced by the unloading related to fluvial erosion.

The integrated approach to such a complex context like continental rifting is essential to understand the role of sub-crustal, crustal, and surface processes in generating regional-scale tectonic structures and relative landscape.

5. Conclusions

In this work, along-axis variations in architecture, segmentation, and evolution of the different sectors of the Main Ethiopian Rift (MER), East Africa, have been analyzed by means of an integrated structural and geomorphological analysis and compared with regional geology and geophysical constraints on lithospheric structure. This analysis suggests the following main conclusions:

1. Approximately 70% of the 500 km long MER is asymmetric, with most asymmetric sectors characterized by a master fault system on the eastern margin. In fact, >70% of the eastern margin is marked by a major boundary fault; the rest is marked by minor faulting and monoclines.
2. The symmetry or asymmetry of the rift is reflected in the topography and hydrography. The rift margin topography gradients differ by <40% in the symmetric portions and >100% in the asymmetric ones. Steep rivers deeply incise the footwall of the major border faults; this erosional unloading increases the isostatic uplift of footwall, enhancing the symmetric/asymmetric topography of each sector of the rift.
3. Rift architecture and segmentation are strongly controlled by the pre-rift lithospheric structure, especially the contrasting nature of the homogeneous, strong Somalian Plateau and the weaker, more heterogeneous Ethiopian Plateau.
4. Asymmetric rift sectors may directly progress to focused axial tectonic-magmatic activity, without transitioning into a symmetric rifting stage.

Acknowledgments
We thank three anonymous reviewers and the Associate Editor Tesfaye Kidane for the detailed comments that helped to improve this manuscript. We also thank Federico Sani for discussions. D.K. is supported by NERC grant NE/L013932/1. The data supporting this paper are listed in the references and available within tables and figures; any further information can be obtained upon request.

References

Abbate, E., Bruni, P., & Sagri, M. (2015). Geology of Ethiopia: A review and geomorphological perspectives. In P. Billi (Ed.), *Landscapes and landforms of Ethiopia, World Geomorphological Landscapes* (pp. 33–64). Dordrecht: Springer Science+Business Media.

Abbate, E., & Sagri, M. (1980). Volcanites of Ethiopian and Somali Plateaus and major tectonic lines. *Atti Convegni Lincei*, *47*, 219–227.

Abdelsalam, M. G., & Stern, R. J. (1996). Sutures and shear zones in the Arabian-Nubian Shield. *Journal of African Earth Sciences*, *23*(3), 289–310. https://doi.org/10.1016/S0899-5362(97)00003-1

Abebe Adhana, T. (2014). The occurrence of a complete continental rift type of volcanic rocks suite along the Yerer–Tullu Wellel Volcano Tectonic Lineament, Central Ethiopia. *Journal of African Earth Sciences*, *99*, 374–385. https://doi.org/10.1016/j.jafrearsci.2014.02.008

Abebe T., Manetti P., Bonini M., Corti G., Innocenti F., Mazzarini F., & Pecskay Z. (2005). Geological map (scale 1:200 000) of the Northern Main Ethiopian Rift and its implication for the volcano-tectonic evolution of the rift. Geological Society of America Maps and Charts, MCH094 (pp. 20).

Abebe, T., Mazzarini, F., Innocenti, F., & Manetti, P. (1998). The Yerer–Tullu Wellel volcanotectonic lineament: A transtentional structure in Central Ethiopia and the associated magmatic activity. *Journal of African Earth Sciences*, *26*(1), 135–150. https://doi.org/10.1016/S0899-5362(97)00141-3

Acocella, V., Korme, T., & Salvini, F. (2003). Formation of normal faults along the axial zone of the Ethiopian rift. *Journal of Structural Geology*, *25*(4), 503–513. https://doi.org/10.1016/S0191-8141(02)00047-0

Agostini, A., Bonini, M., Corti, G., Sani, F., & Manetti, P. (2011). Distribution of quaternary deformation in the central Main Ethiopian Rift, East Africa. *Tectonics*, *30*, TC4010. https://doi.org/10.1029/2010TC002833

Agostini, A., Bonini, M., Corti, G., Sani, F., & Mazzarini, F. (2011). Fault architecture in the Main Ethiopian Rift and comparison with experimental models: Implications for rift evolution and Nubia-Somalia kinematics. *Earth and Planetary Science Letters*, *301*(3-4), 479–492. https://doi.org/10.1016/j.epsl.2010.11.024

Anell, I., Thybo, H., & Artemieva, I. M. (2009). Cenozoic uplift and subsidence in the North Atlantic region: Geological evidence revisited. *Tectonophysics*, *474*(1), 78–105.

Balestrieri, M. L., Bonini, M., Corti, G., Sani, F., & Philippon, M. (2016). A refinement of the chronology of rift-related faulting in the broadly rifted zone, southern Ethiopia, through apatite fission-track analysis. *Tectonophysics*, *671*, 42–55. https://doi.org/10.1016/j.tecto.2016.01.012

Bastow, I. D., Nyblade, A. A., Stuart, G. W., Rooney, T. O., & Benoit, M. H. (2008). Upper mantle seismic structure beneath the Ethiopian hot spot: Rifting at the edge of the African low-velocity anomaly. *Geochemistry, Geophysics, Geosystems*, *9*, Q12022. https://doi.org/10.1029/2008GC002107

Bastow, I. D., Pilidou, S., Kendall, J.-M., & Stuart, G. W. (2010). Melt-induced seismic anisotropy and magma assisted rifting in Ethiopia: Evidence from surface waves. *Geochemistry, Geophysics, Geosystems*, *11*, Q0AB05. https://doi.org/10.1029/2010GC003036

Bastow, I. D., Stuart, G. W., Kendall, J. M., & Ebinger, C. J. (2005). Upper mantle seismic structure in a region of incipient continental breakup: Northern Ethiopian rift. *Geophysical Journal International*, *162*(2), 479–493. https://doi.org/10.1111/j.1365-246X.2005.02666.x

Berhe, S. M. (1990). Ophiolites in northeast and East Africa: Implications for Proterozoic crustal growth. *Journal of the Geological Society of London*, *147*(1), 41–57. https://doi.org/10.1144/gsjgs.147.1.0041

Beutel, E., van Wijk, J., Ebinger, C., Keir, D., & Agostini, A. (2010). Formation and stability of magmatic segments in the Main Ethiopian and Afar Rifts. *Earth and Planetary Science Letters*, *293*, 225–235. https://doi.org/10.1016/j.epsl.2010.02.006

Boccaletti, M., Bonini, M., Mazzuoli, R., Abebe, B., Piccardi, L., & Tortorici, L. (1998). Quaternary oblique extensional tectonics in the Ethiopian Rift (Horn of Africa). *Tectonophysics*, *287*(1-4), 97–116. https://doi.org/10.1016/S0040-1951(98)80063-2

Boccaletti, M., Mazzuoli, R., Bonini, M., Trua, T., & Abebe, B. (1999). Plio-Quaternary volcano-tectonic activity in the northern sector of the Main Ethiopian Rift (MER): Relationships with oblique rifting. *Journal of African Earth Sciences*, *29*(4), 679–698. https://doi.org/10.1016/S0899-5362(99)00124-4

Bonini, M., Corti, G., Innocenti, F., Manetti, P., Mazzarini, F., Abebe, T., & Pecskay, Z. (2005). The evolution of the Main Ethiopian Rift in the frame of Afar and Kenya rifts propagation. *Tectonics*, *24*, TC1007. https://doi.org/10.1029/2004TC001680

Brocklehurst, S. H., & Whipple, K. X. (2002). Glacial erosion and relief production in the eastern sierra Nevada, California. *Geomorphology*, *42*(1-2), 1–24. https://doi.org/10.1016/S0169-555X(01)00069-1

Brune, S. (2016). Rifts and rifted margins: A review of geodynamic processes and natural hazards. In J. C. Duarte & W. P. Schellart (Eds.), *Plate boundaries and natural hazards, Geophysical Monograph Series* (Vol. 219, p. 11–37). Hoboken, NJ: John Wiley.
Buck, W. R. (2017). The role of magmatic loads and rift jumps in generating seaward dipping reflectors on volcanic rifted margins. *Earth and Planetary Science Letters*, *466*, 62–69. https://doi.org/10.1016/j.epsl.2017.02.041
Buiter, S. J. H., & Torsvik, T. H. (2014). A review of Wilson Cycle plate margins: A role for mantle plumes in continental break-up along sutures? *Gondwana Research*, *26*(2), 627–653. https://doi.org/10.1016/j.gr.2014.02.007
Burbank, D. W. (2002). Rates of erosion and their implications for exhumation. *Mineralogical Magazine*, *66*(1), 25–52.
Burov, E., & Cloetingh, S. A. P. L. (1997). Erosion and rift dynamics: New thermomechanical aspects of post-rift evolution of extensional basins. *Earth and Planetary Science Letters*, *150*(1-2), 7–26. https://doi.org/10.1016/S0012-821X(97)00069-1
Casey, M., Ebinger, C. J., Keir, D., Gloaguen, R., & Mohamad, F. (2006). Strain accommodation in transitional rifts: Extension by magma intrusion and faulting in Ethiopian rift magmatic segments. In G. Yirgu, C. J. Ebinger, & P. K. H. Maguire (Eds.), *The Afar Volcanic Province within the East African Rift System Geological Society of London Special Publication* (Vol. 259, pp. 143–163). London, UK: Geological Society Special Publication.
Champagnac, J. D., Schlunegger, F., Norton, K., von Blanckenburg, F., Abbühl, L. M., & Schwab, M. (2009). Erosion-driven uplift of the modern Central Alps. *Tectonophysics*, *474*(1-2), 236–249. https://doi.org/10.1016/j.tecto.2009.02.024
Chorowicz, J. (2005). The east African rift system. *Journal of African Earth Sciences*, *43*(1–3), 379–410. https://doi.org/10.1016/j.jafrearsci.2005.07.019
Cornwell, D. G., Maguire, P. K. H., England, R. W., & Stuart, G. W. (2010). Imaging detailed crustal structure and magmatic intrusion across the Ethiopian Rift using a dense linear broadband array. *Geochemistry, Geophysics, Geosystems*, *11*, Q0AB03. https://doi.org/10.1029/2009GC002637
Corti, G. (2008). Control of rift obliquity on the evolution and segmentation of the main Ethiopian rift. *Nature Geoscience*, *1*(4), 258–262. https://doi.org/10.1038/ngeo160
Corti, G. (2009). Continental rift evolution: From rift initiation to incipient break-up in the Main Ethiopian Rift, East Africa. *Earth Science Reviews*, *96*(1-2), 1–53. https://doi.org/10.1016/j.earscirev.2009.06.005
Corti, G. (2012). Evolution and characteristics of continental rifting: Analogue modeling-inspired view and comparison with examples from the East African Rift System. *Tectonophysics*, *522-523*, 1–33. https://doi.org/10.1016/j.tecto.2011.06.010
Corti, G., Agostini, A., Keir, D., Van Wijk, J., Bastow, I. D., & Ranalli, G. (2015). Magma-induced axial subsidence during final-stage rifting: Implications for the development of seaward dipping reflectors. *Geosphere*, *11*(3), 563–571. https://doi.org/10.1130/GES01076.1
Corti, G., Sani, F., Philippon, M., Sokoutis, D., Willingshofer, E., & Molin, P. (2013). Quaternary volcano-tectonic activity in the Soddo region, western margin of the Southern Main Ethiopian Rift. *Tectonics*, *32*, 861–879.https://doi.org/10.1002/tect.20052
Courtillot, V., Jaupart, C., Manighetti, I., Tapponnier, P., & Besse, J. (1999). On causal links between flood basalts and continental breakup. *Earth and Planetary Science Letters*, *166*, 177–195.
Daly, E., Keir, D., Ebinger, C. J., Stuart, G. W., Bastow, I. D., & Ayele, A. (2008). Crustal tomographic imaging of a transitional continental rift: The Ethiopian rift. *Geophysical Journal International*, *172*(3), 1033–1048. https://doi.org/10.1111/j.1365-246X.2007.03682.x
Daniels, K. A., Bastow, I. D., Keir, D., Sparks, R. S. J., & Menand, T. (2014). Thermal models of dyke intrusion during development of continent–ocean transition. *Earth and Planetary Science Letters*, *385*, 145–153. https://doi.org/10.1016/j.epsl.2013.09.018
Daradich, A., Mitrovica, J. X., Pysklywec, R. N., Willett, S. D., & Forte, A. M. (2003). Mantle flow, dynamic topography, and rift-flank uplift of Arabia. *Geology*, *31*(10), 901–904.
Davidson, A. (1983). The Omo River project: Reconnaissance geology and geochemistry of parts of Illubabor, Kefa, Gemu Gofa, and Sidamo. *Ethiopian Institute Geological Surveys Bulletin*, *2*, 1–89.
Dugda, M. T., Nyblade, A. A., Jordi, J., Langston, C. A., Ammon, C. J., & Simiyu, S. (2005). Crustal structure in Ethiopia and Kenya from receiver function analysis: Implications for rift development in eastern Africa. *Journal of Geophysical Research*, *110*, B01303. https://doi.org/10.1029/2004JB003065
Dunbar, J. A., & Sawyer, D. S. (1989). Continental rifting at pre-existing lithospheric weaknesses. *Nature*, *242*, 565–571.
Ebinger, C. (2005). Continental breakup: The East African perspective. *Astronomy and Geophysics*, *46*, 2.16–2.21.
Ebinger, C. J., & Casey, M. (2001). Continental breakup in magmatic provinces: An Ethiopian example. *Geology*, *29*(6), 527–530. https://doi.org/10.1130/0091-7613(2001)029%3C0527:CBIMPA%3E2.0.CO;2
Ebinger, C. J., Keir, D., Bastow, I. D., Whaler, K., Hammond, J. O. S., Ayele, A., … Hautot, S. (2017). Crustal structure of active deformation zones in Africa: Implications for global crustal processes. *Tectonics*, *36*. https://doi.org/10.1002/2017TC004526
Ebinger, C. J., Yemane, T., Harding, D. J., Tesfaye, S., Kelley, S., & Rex, D. C. (2000). Rift deflection, migration, and propagation: Linkage of the Ethiopian and Eastern rifts, Africa. *Geological Society of America Bulletin*, *112*(2), 163–176. https://doi.org/10.1130/0016-7606(2000)112%3C163:RDMAPL%3E2.0.CO;2
Ebinger, C. J., Yemane, T., WoldeGabriel, G., Aronson, J. L., & Walter, R. C. (1993). Late Eocene-recent volcanism and faulting in the southern main Ethiopian rift. *Journal of the Geological Society of London*, *150*(1), 99–108. https://doi.org/10.1144/gsjgs.150.1.0099
Ethiopian Mapping Agency (1978). *Geological map of the Ethiopia*, *Nazret Sheet*, (scale 1:250.000). Addis Ababa, Ethiopia: Ethiopian Mapping Agency.
Ethiopian Mapping Agency (1981). V. Kazmin & S. M. Berhe (Eds.), *Geological map of the Ethiopian Rift (scale 1:500.000)*. Addis Ababa, Ethiopia: Ethiopian Mapping Agency.
Ethiopian Mapping Authority (1996). *Geological map of Ethiopia (scale 1:2.000.000)*. Addis Ababa, Ethiopia: Ethiopian Mapping Authority.
Flint, J. J. (1974). Stream gradient as a function of order, magnitude, and discharge. *Water Resources Research*, *10*, 969–973. https://doi.org/10.1029/WR010i005p00969
Gallacher, R. J., Keir, D., Harmon, N., Stuart, G., Leroy, S., Hammond, J. O., … Ahmed, A. (2016). The initiation of segmented buoyancy-driven melting during continental breakup. *Nature Communications*, *7*, 13110. https://doi.org/10.1038/ncomms13110
Gani, N. D., Abdelsalam, M. G., & Gani, M. R. (2007). Blue Nile incision on the Ethiopian Plateau: Pulsed plateau growth, Pliocene uplift, and hominin evolution. *GSA Today*, *17*(9), 4–11. https://doi.org/10.1130/GSAT01709A.1
Gashawbeza, E. M., Klemperer, S. L., Nyblade, A. A., Walker, K. T., & Keranen, K. M. (2004). Shear-wave splitting in Ethiopia: Precambrian mantle anisotropy locally modified by Neogene rifting. *Geophysical Research Letters*, *31*, L18602. https://doi.org/10.1029/2004GL020471
Gouin, P. (1979). *Earthquake history of Ethiopia and the Horn of Africa* (p. 258). Ottawa: IDRC.
Grimmer, J. C., Ritter, J. R. R., Eisbacher, G. H., & Fielitz, V. (2017). The Late Variscan control on the location and asymmetry of the Upper Rhine Graben. *International Journal of Earth Sciences (Geol Rundsch)*, *106*(3), 827–853. https://doi.org/10.1007/s00531-016-1336-x
Hack, J. T. (1957). *Studies of longitudinal profiles in Virginia and Maryland*, *U. S. Geological Survey Professional Paper* (Vol. 294, pp. 45–97). Washington, DC: U.S. Government Printing Office.

Hayward, N. J., & Ebinger, C. J. (1996). Variations in the along-axis segmentation of the Afar Rift system. *Tectonics*, *15*, 244–257. https://doi.org/10.1029/95TC02292

Howard, A. D., Dietrich, W. E., & Seidl, M. A. (1994). Modeling fluvial erosion on regional to continental scales. *Journal of Geophysical Research: Solid Earth*, *99*, 13,971–13,986.

Huismans, R. S., & Beaumont, C. (2005). Effect of lithospheric stratification on extensional styles and rift basin geometry. In *Petroleum systems of divergent margin basins, 25th gulf coast section, Society Sedimentary Geology, Bob F. Perkins Research Conference* (pp. 4–7). Houston, TX.

Huismans, R. S., & Beaumont, C. (2014). Rifted continental margins: The case for depth-dependent extension. *Earth and Planetary Science Letters*, *407*, 148–162. https://doi.org/10.1016/j.epsl.2014.09.032

Hutchison, W., Mather, T. A., Pyle, D. M., Biggs, J., & Yirgu, G. (2015). Structural controls on fluid pathways in an active rift system: A case study of the Aluto volcanic complex. *Geosphere*, *11*(3), 542–562. https://doi.org/10.1130/GES01119.1

Isacks, B. L. (1992). Long term land surface processes: Erosion, tectonics and climate history in mountain belts. In P. Mather (Ed.), *TERRA-1: Understanding the terrestrial environment* (pp. 21–36). London, UK: Taylor and Francis.

Kazmin, V., Seife, M. B., Nicoletti, M., & Petrucciani, C. (1980). Evolution of the northern part of the Ethiopian rift. Geodynamic Evolution of the Afro-Arabian Rift System, Accademia Nazionale Dei Lincei, Atti dei Convegni Lincei 47 (pp. 275–292).

Kazmin, V., Shifferaw, A., & Balcha, T. (1978). The Ethiopian basement: Stratigraphy and possible manner of evolution. International Journal of Earth Sciences. *Geologische Rundschau*, *67*(2), 531–546. https://doi.org/10.1007/BF01802803

Keir, D., Bastow, I., Pagli, C., & Chambers, E. (2013). The development of extension and magmatism in the Red Sea rift of Afar. *Tectonophysics*, *607*, 98–114. https://doi.org/10.1016/j.tecto.2012.10.015

Keir, D., Bastow, I. D., Corti, G., Mazzarini, F., & Rooney, T. O. (2015). The origin of along-rift variations in faulting and magmatism in the Ethiopian rift. *Tectonics*, *34*, 464–477. https://doi.org/10.1002/2014TC003698

Keir, D., Ebinger, C. J., Stuart, G. W., Daly, E., & Ayele, A. (2006). Strain accommodation by magmatism and faulting as rifting proceeds to breakup: Seismicity of the northern Ethiopian rift. *Journal of Geophysical Research*, *111*, B05314. https://doi.org/10.1029/2005JB003748

Kendall, J. M., Stuart, G. W., Ebinger, C. J., Bastow, I. D., & Keir, D. (2005). Magma assisted rifting in Ethiopia. *Nature*, *433*(7022), 146–148. https://doi.org/10.1038/nature03161

Keranen, K., & Klemperer, S. L. (2008). Discontinuous and diachronous evolution of the Main Ethiopian Rift: Implications for the development of continental rifts. *Earth and Planetary Science Letters*, *265*(1-2), 96–111. https://doi.org/10.1016/j.epsl.2007.09.038

Keranen, K., Klemperer, S. L., Gloaguen, R., & Eagle Working Group (2004). Three-dimensional seismic imaging of a protoridge axis in the Main Ethiopian rift. *Geology*, *32*, 949–952.

Keranen, K., Klemperer, S. L., Julia, J., Lawrence, J. L., & Nyblade, A. (2009). Low lower-crustal velocity across Ethiopia: Is the Main Ethiopian Rift a narrow rift in a hot craton? *Geochemistry, Geophysics, Geosystems*, *10*, Q0AB01. https://doi.org/10.1029/2008GC002293

Kirby, E., Johnson, C., Furlong, K., & Heimsath, A. (2007). Transient channel incision along Bolinas Ridge, California: Evidence for differential rock uplift adjacent to the San Andreas fault. *Journal of Geophysical Research*, *112*, F03S07. https://doi.org/10.1029/2006JF000559

Kirby, E., & Whipple, K. X. (2001). Quantifying differential rock-uplift rates via stream profile analysis. *Geology*, *29*(5), 415–418. https://doi.org/10.1130/0091-7613(2001)029%3C0415:QDRURV%3E2.0.CO;2

Kobor, J. S., & Roering, J. J. (2004). Systematic variation of bedrock channel gradients in the central Oregon Coast Range: Implications for rock uplift and shallow landsliding. *Geomorphology*, *62*(3-4), 239–256. https://doi.org/10.1016/j.geomorph.2004.02.013

Kogan, L., Fisseha, S., Bendick, R., Reilinger, R., McClusky, S., King, R., & Solomon, T. (2012). Lithospheric strength and strain localization in continental extension from observations of the East African Rift. *Journal of Geophysical Research*, *117*, B03402. https://doi.org/10.1029/2011JB008516

Kooi, H., & Beaumont, C. (1994). Escarpment evolution on high-elevation rifted margins: Insights derived from a surface processes model that combines diffusion, advection, and reaction. *Journal of Geophysical Research*, *99*, 12,191–12,209. https://doi.org/10.1029/94JB00047

Korme, T., Acocella, V., & Abebe, B. (2004). The role of pre-existing structures in the origin, propagation and architecture of faults in the Main Ethiopian Rift. *Gondwana Research*, *7*(2), 467–479. https://doi.org/10.1016/S1342-937X(05)70798-X

Laó-Dávila, D. A., Al-Salmi, H. S., Abdelsalam, M. G., & Atekwana, E. A. (2015). Hierarchical segmentation of the Malawi Rift: The influence of inherited lithospheric heterogeneity and kinematics in the evolution of continental rifts. *Tectonics*, *34*, 2399–2417. https://doi.org/10.1002/2015TC003953

Lock, J., Kelsey, H., Furlong, K., & Woolace, A. (2006). Late Neogene and Quaternary landscape evolution of the Northern California Coast Ranges: Evidence for Mendocino triple junction tectonics. *Geological Society of America Bulletin*, *118*(9-10), 1232–1246. https://doi.org/10.1130/B25885.1

Mackenzie, G. H., Thybo, G. H., & Maguire, P. (2005). Crustal velocity structure across the Main Ethiopian Rift: results from 2-dimenional wide-angle seismic modeling. *Geophysical Journal International*, *162*, 994–1006. https://doi.org/10.1111/j.1365-246X.2005.02710.x

Maguire, P. K. H., Keller, G. R., Klemperer, S. L., Mackenzie, G. D., Keranen, K., Harder, S., … Amha, M. (2006). Crustal structure of the Northern Main Ethiopian Rift from the EAGLE controlled source survey; a snapshot of incipient lithospheric break-up. In G. Yirgu, C. J. Ebinger, & P. K. H. Maguire (Eds.), *The Afar volcanic province within the East African Rift System*, *Geological Societyof London, Special Publication* (Vol. 259, pp. 269–291). London, UK.

Mohr, P. (1962). The Ethiopian Rift System. *Bulletin of the Geophysical Observatory of Addis Ababa*, *5*, 33–62.

Mohr, P. (1983). Volcanotectonic aspects of the Ethiopian Rift evolution. *Bulletin Centre Recherches Elf Aquitaine Exploration Production*, *7*, 175–189.

Molin, P., & Corti, G. (2015). Topography, river network and recent fault activity at the margins of the central main Ethiopian rift (East Africa). *Tectonophysics*, *664*, 67–82. https://doi.org/10.1016/j.tecto.2015.08.045

Molin, P., Pazzaglia, F. J., & Dramis, F. (2004). Geomorphic expression of active tectonics in a rapidly deforming forearc, Sila Massif, Calabria, southern Italy. *American Journal of Science*, *304*(7), 559–589. https://doi.org/10.2475/ajs.304.7.559

Molnar, P., & England, P. (1990). Late Cenozoic uplift of mountain ranges and global climate change: Chicken or egg? *Nature*, *346*(6279), 29–34. https://doi.org/10.1038/346029a0

Mueller, K., Kier, G., Rockwell, T., & Jones, C. H. (2009). Quaternary rift flank uplift of the Peninsular Ranges in Baja and southern California by removal of mantle lithosphere. *Tectonics*, *28*, TC5003. https://doi.org/10.1029/2007TC002227

Müller, R. D., Cande, S. C., Stock, J. M., & Keller, W. R. (2005). Crustal structure and rift flank uplift of the Adare Trough, Antarctica. *Geochemistry, Geophysics, Geosystems*, *6*, Q11010. https://doi.org/10.1029/2005GC001027

Pazzaglia, F. J., & Gardner, T. W. (1994). Late Cenozoic flexural deformation of the middle US Atlantic passive margin. *Journal of Geophysical Research: Solid Earth*, *99*, 12,143–12,157.

Pazzaglia, F. J., Gardner, T. W., & Merritts, D. J. (1998). Bedrock fluvial incision and longitudinal profile development over geologic time scales determined by fluvial terraces. In E. Wohl & K. Tinkler (Eds.), *River over rock: Fluvial processes in bedrock channels, Geophysical Monograph Series* (Vol. 107, pp. 207–235). Washington, DC: American Geophysical Union. https://doi.org/10.1029/GM107p0207

Pérez-Gussinyé, M., Metois, M., Fernández, M., Vergés, J., Fullea, J., & Lowry, A. R. (2009). Effective elastic thickness of Africa and its relationship to other proxies for lithospheric structure and surface tectonics. *Earth and Planetary Science Letters*, *287*(1-2), 152–167. https://doi.org/10.1016/j.epsl.2009.08.004

Petit, C., Fournier, M., & Gunnell, Y. (2007). Tectonic and climatic controls on rift escarpments: Erosion and flexural rebound of the Dhofar passive margin (Gulf of Aden, Oman). *Journal of Geophysical Research*, *112*, B03406. https://doi.org/10.1029/2006JB004554

Philippon, M., Corti, G., Sani, F., Bonini, M., Balestrieri, M. L., Molin, P., … Cloetingh, S. (2014). Evolution, distribution and characteristics of rifting in southern Ethiopia. *Tectonics*, *33*, 485–508. https://doi.org/10.1002/2013TC003430

Pik, R., Marty, B., Carignan, J., Yirgu, G., & Ayalew, T. (2008). Timing of East African Rift development in southern Ethiopia: Implication for mantle plume activity and evolution of topography. *Geology*, *36*(2), 167–170. https://doi.org/10.1130/G24233A.1

Pizzi, A., Coltorti, M., Abebe, B., Disperati, L., Sacchi, G., & Salvini, R. (2006). The Wonji fault belt (Main Ethiopian Rift): Structural and geomorphological constraints and GPS monitoring. In G. Yirgu, C. J. Ebinger, & P. K. H. Maguire (Eds.), *The Afar volcanic province within the East African Rift System*, *Geological Society of London, Special Publication* (Vol. 259, pp. 191–207). London, UK.

Ponza, A., Pazzaglia, F. J., & Picotti, V. (2010). Thrust-fold activity at the mountain front of the Northern Apennines (Italy) from quantitative landscape analysis. *Geomorphology*, *123*(3-4), 211–231. https://doi.org/10.1016/j.geomorph.2010.06.008

Poulimenos, G., & Doutsos, T. (1997). Flexural uplift of rift flanks in central Greece. *Tectonics*, *16*(6), 912–923.

Ring, U. (1994). The influence of preexisting structure on the evolution of the Cenozoic Malawi Rift (East African Rift System). *Tectonics*, *13*, 313–326. https://doi.org/10.1029/93TC03188

Ritsema, J., van Heijst, H. J., & Woodhouse, J. H. (1999). Complex shear wave velocity structure imaged beneath Africa and Iceland. *Science*, *286*(5446), 1925–1928. https://doi.org/10.1126/science.286.5446.1925

Rooney, T. O. (2010). Geochemical evidence of lithospheric thinning in the southern Main Ethiopian Rift. *Lithos*, *117*(1-4), 33–48. https://doi.org/10.1016/j.lithos.2010.02.002

Saria, E., Calais, E., Stamps, D. S., Delvaux, D., & Hartnady, C. J. H. (2014). Present-day kinematics of the East African Rift. *Journal of Geophysical Research*, *119*, 3584–3600. https://doi.org/10.1002/2013JB010901

Scholz, C. H., & Contreras, J. C. (1998). Mechanics of continental rift architecture. *Geology*, *26*(11), 967–970. https://doi.org/10.1130/0091-7613(1998)026%3C0967:MOCRA%3E2.3.CO;2

Schorghofer, N., & Rothman, D. H. (2002). A causal relations between topographic slope and drainage area. *Geophysical Research Letters*, *29*(13), 1633. https://doi.org/10.1029/2002GL015144

Scotti, V. N., Molin, P., Faccenna, C., Soligo, M., & Casas-Sainz, A. (2013). The influence of surface and tectonic processes on landscape evolution of the Iberian Chain (Spain): Quantitative geomorphological analysis and geochronology. *Geomorphology*, *206*, 37–57. https://doi.org/10.1016/j.geomorph.2013.09.017

Sembroni, A., Faccenna, C., Becker, T. W., Molin, P., & Bekele, A. (2016). Long term, deep mantle support of the Ethiopia-Yemen Plateau. *Tectonics*, *35*, 469–488. https://doi.org/10.1002/2015TC004000

Sembroni, A., Molin, P., Pazzaglia, F. J., Faccenna, C., & Bekele, A. (2016). Evolution of continental-scale drainage in response to mantle dynamics and surface processes: An example from the Ethiopian Highlands. *Geomorphology*, *261*, 12–29. https://doi.org/10.1016/j.geomorph.2016.02.022

Sklar, L. S., & Dietrich, W. E. (1998). River longitudinal profiles and bedrock incision models: Stream power and the influence of sediment supply. In K. Tinkler & E. E. Wohl (Eds.), *Rivers over rock: Fluvial processes in Bedrock Channels*, *Geophysical Monograph Series* (Vol. 107, pp. 237–260). John Wiley. https://doi.org/10.1029/GM107p0237

Snyder, N., Whipple, K. X., Tucker, G. E., & Merritts, D. J. (2000). Landscape response to tectonic forcing: Digital elevation model analysis of stream profiles in the Mendocino triple junction region, northern California. *Geological Society of America Bulletin*, *112*(8), 1250–1263. https://doi.org/10.1130/0016-7606(2000)112%3C1250:LRTTFD%3E2.0.CO;2

Sokoutis, D., Corti, G., Bonini, M., Brun, J.-P., Cloetingh, S., Mauduit, T., & Manetti, P. (2007). Modelling the extension of heterogeneous hot lithosphere. *Tectonophysics*, *444*(1-4), 63–79. https://doi.org/10.1016/j.tecto.2007.08.012

Stern, R. J. (2002). Crustal evolution in the East African Orogen: A neodymium isotopic perspective. *Journal of African Earth Sciences*, *34*(3-4), 109–117. https://doi.org/10.1016/S0899-5362(02)00012-X

Stern, R. J., Nielsen, K. C., Best, E., Sultan, M., Arvidson, R. E., & Kroner, A. (1990). Orientation of the late Precambrian sutures in the Arabian-Nubian Shield. *Geology*, *18*(11), 1103–1106. https://doi.org/10.1130/0091-7613(1990)018%3C1103:OOLPSI%3E2.3.CO;2

Stern, T. A., Baxter, A. K., & Barrett, P. J. (2005). Isostatic rebound due to glacial erosion within the Transantarctic Mountains. *Geology*, *33*(3), 221–224. https://doi.org/10.1130/G21068.1

Stern, T. A., & ten Brink, U. S. (1989). Flexural uplift of the Transantarctic Mountains. *Journal of Geophysical Research*, *94*(B8), 10,315–10,330.

Stuart, G. W., Bastow, I. D., & Ebinger, C J. (2006). Crustal structure of the northern main Ethiopian Rift from receiver function studies. In G. Yirgu, C. J. Ebinger, & P. K. H. Maguire (Eds.), *The Afar volcanic province within the East African Rift System*, *Geological Society of London, Special Publication* (Vol. 259, pp. 253–267). London, UK.

Tarboton, D. G., Bras, R. L., & Rodríguez-Iturbe, I. (1989). Scaling and elevation in river networks. *Water Resources Research*, *25*, 2037–2051. https://doi.org/10.1029/WR025i009p02037

Tomkin, J. H., Brandon, M. T., Pazzaglia, F. J., Barbour, J. R., & Willett, S. D. (2003). Quantitative testing of bedrock incision models, Clearwater River, NW Washington State. *Journal of Geophysical Research*, *108*(B6), 2308. https://doi.org/10.1029/2001JB000862

Tommasi, A., & Vauchez, A. (2001). Continental rifting parallel to ancient collisional belts: An effect of the mechanical anisotropy of the lithospheric mantle. *Earth and Planetary Science Letters*, *185*(1-2), 199–210. https://doi.org/10.1016/S0012-821X(00)00350-2

Tucker, G. E., & Slingerland, R. L. (1994). Erosional dynamics, flexural isostasy, and long-lived escarpments: A numerical modeling study. *Journal of Geophysical Research*, *99*, 12,229–12,243. https://doi.org/10.1029/94JB00320

Vail, J. R. (1983). Pan-African crustal accretion in north-east Africa. *Journal of African Earth Sciences*, *1*, 285–294.

Vauchez, A., Barruol, G., & Tommasi, A. (1997). Why do continents break-up parallel to ancient orogenic belts? *Terra Nova*, *9*(2), 62–66. https://doi.org/10.1111/j.1365-3121.1997.tb00003.x

Versfelt, J., & Rosendahl, B. R. (1989). Relationships between pre-rift structure and rift architecture in Lakes Tanganyika and Malawi: East Africa. *Nature*, *337*(6205), 354–357. https://doi.org/10.1038/337354a0

Wegmann, K. W., & Pazzaglia, F. J. (2002). Holocene strath terraces, climate change, and active tectonics: The Clearwater River basin, Olympic Peninsula, Washington State. *Geological Society of America Bulletin*, *114*(6), 731–744. https://doi.org/10.1130/0016-7606(2002)114%3C0731:HSTCCA%3E2.0.CO;2

Weissel, J., Malinverno, A., & Harding, D. (1995). Erosional development of the Ethiopian Plateau of Northeast Africa from fractal analysis of topography. In C. C. Barton & P. R. Pointe (Eds.), *Fractals in Petroleum Geology and Earth Processes* (pp. 127–142). New York: Plenum Press. https://doi.org/10.1007/978-1-4615-1815-0_8

Weissel, J. K., & Karner, G. D. (1989). Flexural uplift of rift flanks due to mechanical unloading of the lithosphere during extension. *Journal of Geophysical Research*, *94*, 13,919–13,950. https://doi.org/10.1029/JB094iB10p13919

Wernicke, B. (1985). Uniform-sense simple shear of the continental lithosphere. *Canadian Journal of Earth Sciences*, *32*, 108–125.

Whaler, K. A., & Hautot, S. (2006). The electrical resistivity structure of the crust beneath the northern Main Ethiopian Rift. In G. Yirgu, C. J. Ebinger, & P. K. H. Maguire (Eds.), *The Afar volcanic province within the East African Rift System*, *Geological Society of London, Special Publication* (Vol. 259, pp. 293–305). London, UK.

Whipple, K. X. (2004). Bedrock rivers and the geomorphology of active orogens. *Annual Review of Earth and Planetary Sciences*, *32*(1), 151–185. https://doi.org/10.1146/annurev.earth.32.101802.120356

Whipple, K. X., Hancock, G. S., & Anderson, R. S. (2000). River incision into bedrock: Mechanicsand relative efficacy of plucking, abrasion, and cavitation. *Geological Society of America Bulletin*, *112*(3), 490–503. https://doi.org/10.1130/0016-7606(2000)112%3C490:RIIBMA%3E2.0.CO;2

Whipple, K. X., & Tucker, G. E. (1999). Dynamics of the stream-power river incision model: Implications for height limits of mountain ranges, landscape response timescales, and research needs. *Journal of Geophysical Research*, *104*, 17,661–17,674. https://doi.org/10.1029/1999JB900120

Whipple, K. X., Wobus, C., Crosby, B., Kirby, E., & Sheehan, D. (2007). New tools for quantitative geomorphology: Extraction and interpretation of stream profiles from digital topographic data. Geological Society of America Annual Meeting, Short Course Guide, Denver. Retrieved from http://www.geomorphtools.org

Willett, S. D. (1999). Orogeny and orography: The effects of erosion on the structure of mountain belts. *Journal of Geophysical Research*, *104*(B12), 28,957–28,981.

Willett, S. D., Slingerland, R., & Hovius, N. (2001). Uplift, shortening and steady state topography in active mountain belts. *American Journal of Science*, *301*, 455–485.

Wittmann, H., von Blanckenburg, F., Kruesmann, T., Norton, K. P., & Kubik, P. W. (2007). Relation between rock uplift and denudation from cosmogenic nuclides in river sediment in the Central Alps of Switzerland. *Journal of Geophysical Research*, *112*, F04010. https://doi.org/10.1029/2006JF000729

Wobus, C., Whipple, K. X., Kirby, E., Snyder, N., Johnson, J., Spyropolou, K., … Sheehan, D. (2006). Tectonics from topography: Procedures, promise, and pitfalls. In S. Willett, et al. (Eds.), *Tectonics, climate, and landscape evolution*, *Geological Society of America Special Papers* (Vol. 398, pp. 55–74). Boulder, CO: Geological Society of America.

WoldeGabriel, G., Aronson, J. L., & Walter, R. C. (1990). Geology, geochronology, and rift basin development in the central sector of the Main Ethiopia Rift. *Geological Society of America Bulletin*, *102*, 439–458.

Wolfenden, E., Ebinger, C., Yirgu, G., Deino, A., & Ayale, D. (2004). Evolution of the northern Main Ethiopian rift: Birth of a triple junction. *Earth and Planetary Science Letters*, *224*(1-2), 213–228. https://doi.org/10.1016/j.epsl.2004.04.022

Ziegler, P. A., & Cloetingh, S. (2004). Dynamic processes controlling evolution of rifted basins. *Earth Science Reviews*, *64*(1-2), 1–50. https://doi.org/10.1016/S0012-8252(03)00041-2